

AD-A134 636

MASS SPECTROMETRIC DECOMPOSITION STUDIES ON SEVERAL  
AZIDO AND NITRATO POL..(U) SPACE SCIENCES INC MONROVIA  
CA M FARBER ET AL SEP 83 N00014-80-C-0711

1/1

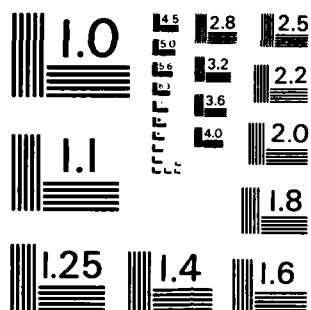
UNCLASSIFIED

F/G 7/4

NL

END  
DATE  
FILMED

12  
DTIC



MICROCOPY RESOLUTION TEST CHART  
NATIONAL BUREAU OF STANDARDS-1963-A

2  
**SPACE SCIENCES, INC.**

135 WEST MAPLE AVENUE • MONROVIA, CALIFORNIA 91016 • (213) 357-3879

AD-A134 636

**MASS SPECTROMETRIC THERMAL DECOMPOSITION STUDIES ON  
SEVERAL AZIDO AND NITRATO POLYMERS, THERMAL  
PLASTICIZERS AND NOVEL NITRAMINES**

Milton Farber, S. P. Harris and R. D. Srivastava

**ANNUAL SUMMARY REPORT**

Department of the Navy  
Office of Naval Research  
Arlington, Virginia 22217

September 1983

NOV 14 1983

A

DTIC FILE COPY

Approved for public release; distribution unlimited.  
Reproduction in whole or in part is permitted for  
any purpose by the United States Government.  
This research was sponsored by the Office of Naval  
Research.

8. 1

034

UNCLASSIFIED

SECURITY CLASSIFICATION OF THIS PAGE (When Data Entered)

REPORT DOCUMENTATION PAGE		READ INSTRUCTIONS BEFORE COMPLETING FORM
1. REPORT NUMBER	2. GOVT ACCESSION NO. AD-A134 6	3. RECIPIENT'S CATALOG NUMBER 36
4. TITLE (and Subtitle) Mass Spectrometric Decomposition Studies on Several Azido and Nitrate Polymers, Thermal Plasticizers and Novel Nitramines		5. TYPE OF REPORT & PERIOD COVERED Annual Summary 1 Aug 1982 - 31 July 1983
		6. PERFORMING ORG. REPORT NUMBER
7. AUTHOR(s) Milton Farber, S. P. Harris and R. D. Srivastava		8. CONTRACT OR GRANT NUMBER(s) N00014-80-C-0711
9. PERFORMING ORGANIZATION NAME AND ADDRESS Space Sciences, Inc. 135 W. Maple Ave. Monrovia, CA 91016		10. PROGRAM ELEMENT, PROJECT, TASK AREA & WORK UNIT NUMBERS
11. CONTROLLING OFFICE NAME AND ADDRESS Office of Naval Research (Code 432) Arlington, Virginia 22217		12. REPORT DATE September 1983
		13. NUMBER OF PAGES 54
14. MONITORING AGENCY NAME & ADDRESS (if different from Controlling Office)		15. SECURITY CLASS. (of this report) Unclassified
		15a. DECLASSIFICATION/DOWNGRADING SCHEDULE
16. DISTRIBUTION STATEMENT (of this Report) Approved for public release; distribution unlimited.		
17. DISTRIBUTION STATEMENT (of the abstract entered in Block 20, if different from Report)		
18. SUPPLEMENTARY NOTES		
19. KEY WORDS (Continue on reverse side if necessary and identify by block number) bis azido methyl oxetane (BAMO)      bis ethoxy methyl oxetane (BEMO) azido methyl methyl oxetane (AMMO)      bis fluoro methyl oxetane (BFMO) azido oxetane (AZOX)      thermal decomposition bis nitrate methyl oxetane (BNMO)      activation energies glycidyl azide polymer (GAP)      mass spectrometry      copolymers		
20. ABSTRACT (Continue on reverse side if necessary and identify by block number) → Effusion mass spectrometric investigation of BAMO, AMMO, AZOX and GAP yielded primary decomposition of N <sub>2</sub> release at approximately 120 C and E <sub>a</sub> values of 170 - 180 kJ mol <sup>-1</sup> (43 - 43 kcal mol <sup>-1</sup> ). The 50-50% copolymer of BAMO-BNMO decomposes initially through the nitrate constituent at approximately 100 C followed by the azide decomposition. The thermal degradation mechanism for BEMO appears to be a stepwise breaking of the ethoxy-methyl bonds followed by the stripping of the methylene groups. BFMO is stable to temperatures greater than 200 C →		

DD FORM 1 JAN 73 1473 EDITION OF 1 NOV 65 IS OBSOLETE

UNCLASSIFIED

SECURITY CLASSIFICATION OF THIS PAGE (When Data Entered)

UNCLASSIFIED

SECURITY CLASSIFICATION OF THIS PAGE(When Data Entered)

→ with initial decomposition products of HF, with considerable depolymerization occurring. The major decomposition product of the NSWG novel nitramine,  $C_6H_8N_8O_{12}$ , is the eight-membered nitramine ring less two  $NO_2$  molecules, molecular weight 292. The decomposition product is stable in the gas phase at 300 C. —



UNCLASSIFIED

SECURITY CLASSIFICATION OF THIS PAGE(When Data Entered)

## I. INTRODUCTION

Thermal decomposition studies were performed by effusion-mass spectrometry on a number of propellant materials, including azido polymers, nitrato polymers, thermal plasticizers and novel nitramines.

The azido polymers included formulations of BAMO, AMMO and AZOX synthesized by Dr. G. E. Manser of Morton Thiokol Wasatch Division, and GAP, prepared by Dr. M. B. Frankel of the Rocketdyne Division of Rockwell International. The nitrato compounds included BNMO supplied by Dr. Manser and TMETN prepared by Dr. Russell Reed of the Naval Ordnance Test Station, China Lake. Samples of two thermal plasticizers, BEMO and BFMO, also were supplied by Dr. Manser. A novel nitramine was furnished by Dr. Horst Adolph of the White Oak Naval Surface Weapons Center.

Reaction kinetics and mechanisms were proposed from the mass spectra obtained for the degradation products and are discussed in the following sections of this report.

## II. MASS SPECTROMETER STUDIES

### A. Thermal Decomposition of Azido Polymers

A paper entitled "Mass Spectrometric Kinetic Studies on Several Azido Polymers" coauthored by Milton Farber, S. P. Harris, and R. D. Srivastava will appear in "Combustion and Flame" in the near future. A preprint of the paper is presented in Appendix A.

### B. Thermal Decomposition of Nitrato Compounds

#### 1. Thermal Decomposition of the 50-50% BAMO-BNMO Copolymer

The 50-50% BAMO-BNMO copolymer was purified for approximately 60 hours in vacuum at 60 C. This removed all traces of the solvent methylene chloride (less than one part in  $10^6$  as seen with the mass spectrometer). The purified copolymer appears to be stable to nearly 100 C, as can be seen from Fig. 1, which shows small concentrations of  $\text{NO}_2$  at that temperature. Upon heating the copolymer to 150 C the BAMO constituent begins to decompose, with the release of 44 amu fragments, presumably  $\text{C}_2\text{H}_4\text{O}$  and  $\text{CO}_2$ . At 170 C the decomposition of BAMO has increased to where the 44 amu concentration is greater than that of the  $\text{NO}_2$  from the BNMO constituent.

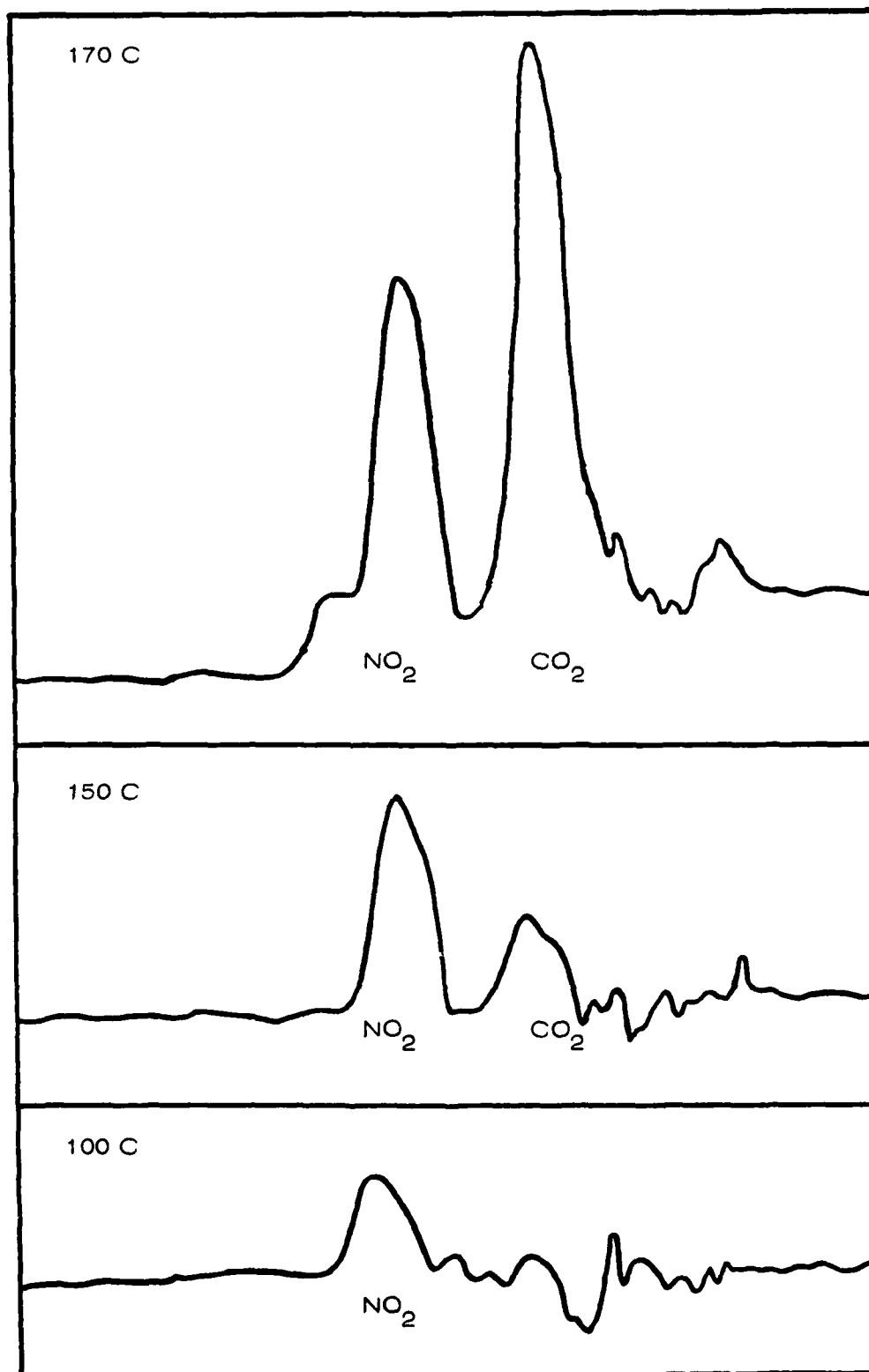


Fig. 1. Relative  $\text{NO}_2$  and  $\text{CO}_2$  comparison as a function of temperature for decomposition of 50-50% BAMO-BNMO

Figure 2 compares the rate of decomposition of the two polymers which make up the copolymer at three temperatures. This figure clearly shows the dramatic change in decomposition rates of the various species in the 14 to 50 amu range as the temperature is increased from 140 to 200 C.

## 2. Unstabilized TMETN

In order to compare the thermal decomposition characteristics of the BAMO-BNMO copolymer, studies were made on a nitrated plasticizer, trimethyl ethane trinitrate (TMETN), unstabilized. However, such a comparison should be considered as very qualitative since these are two entirely different classes of compounds; i.e., a monomer against a polymer, although both contain  $\text{ONO}_2$  groups. Figure 3 shows the mass peaks resulting from the heating of TMETN in vacuum arriving at the mass spectrometer at a fairly low temperature, 50 C. The mass fragments are similar to those of BNMO, although they are observed at lower temperatures.

## C. Degradation of Thermal Plasticizers

### 1. Thermal Decomposition of BEMO

A combined three-laboratory research program was undertaken to investigate bis (ethoxy methyl) oxetane, BEMO. Synthesis and TGA analyses were performed at Morton Thiokol Wasatch Division by Dr. G. E. Manser's group. Thermal degradation and mechanistic studies were conducted by Professor L. H. Sperling's group at Lehigh University, and the mass spectrometric thermal decomposition investigations were performed at Space Sciences, Inc. A joint paper is being prepared for publication in an appropriate polymer journal.

A melting point for BEMO of  $80 \pm 2$  C was determined in vacuum. This polymer is stable to approximately 200 C. However, at 150 C very small concentrations of decomposition products are seen. Figure 4 shows mass spectra at three isothermal temperatures, 100, 150 and 200 C. As can be seen, at 150 C there are three definite regions of decomposition products, 56, 70, and 84 amu. At 200 C decomposition is slightly more pronounced but appears to be in the same spectral region.



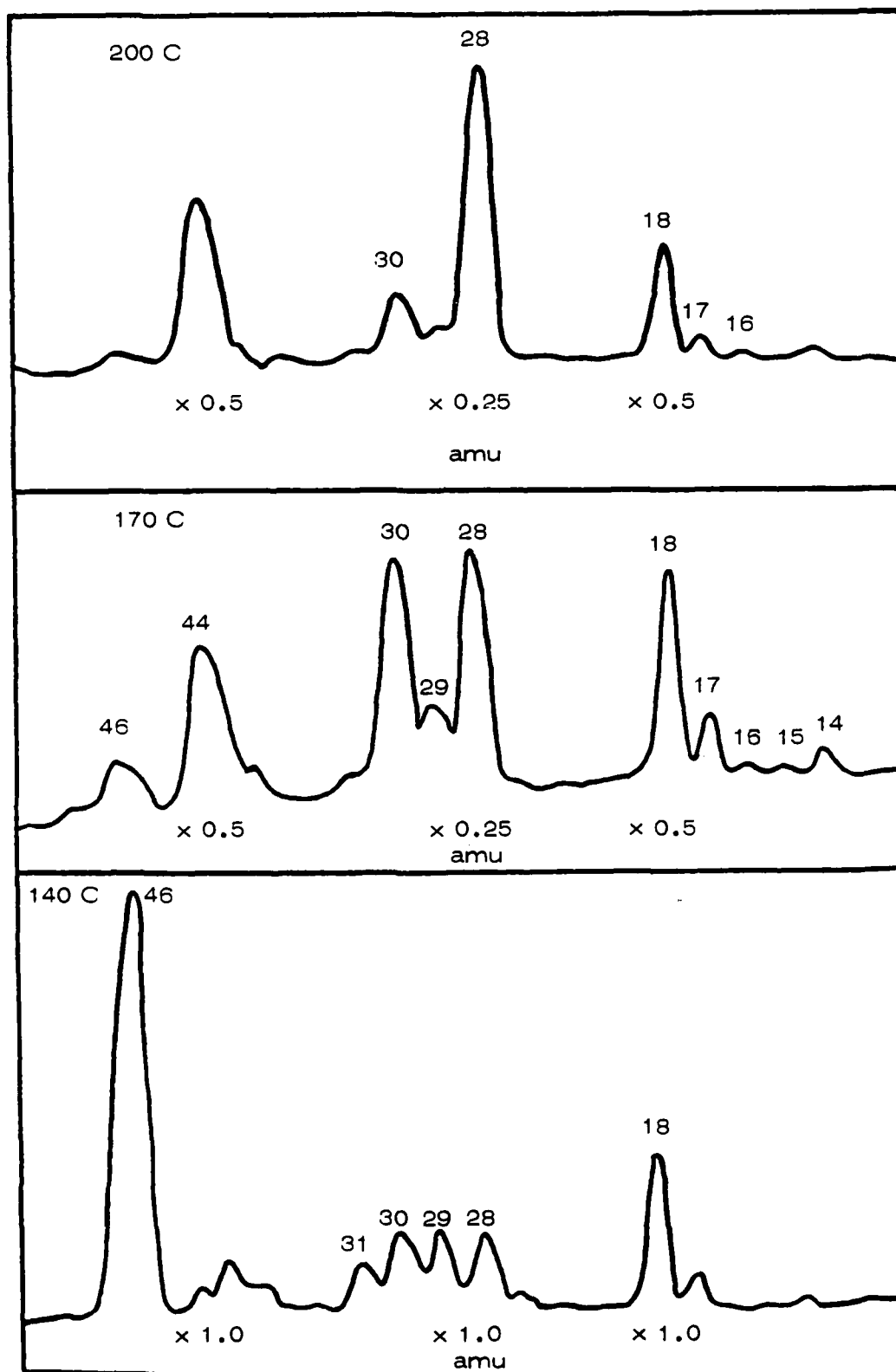


Fig. 2. Thermal decomposition of 50-50% BAMO-BNMO as a function of three temperatures in three amu ranges

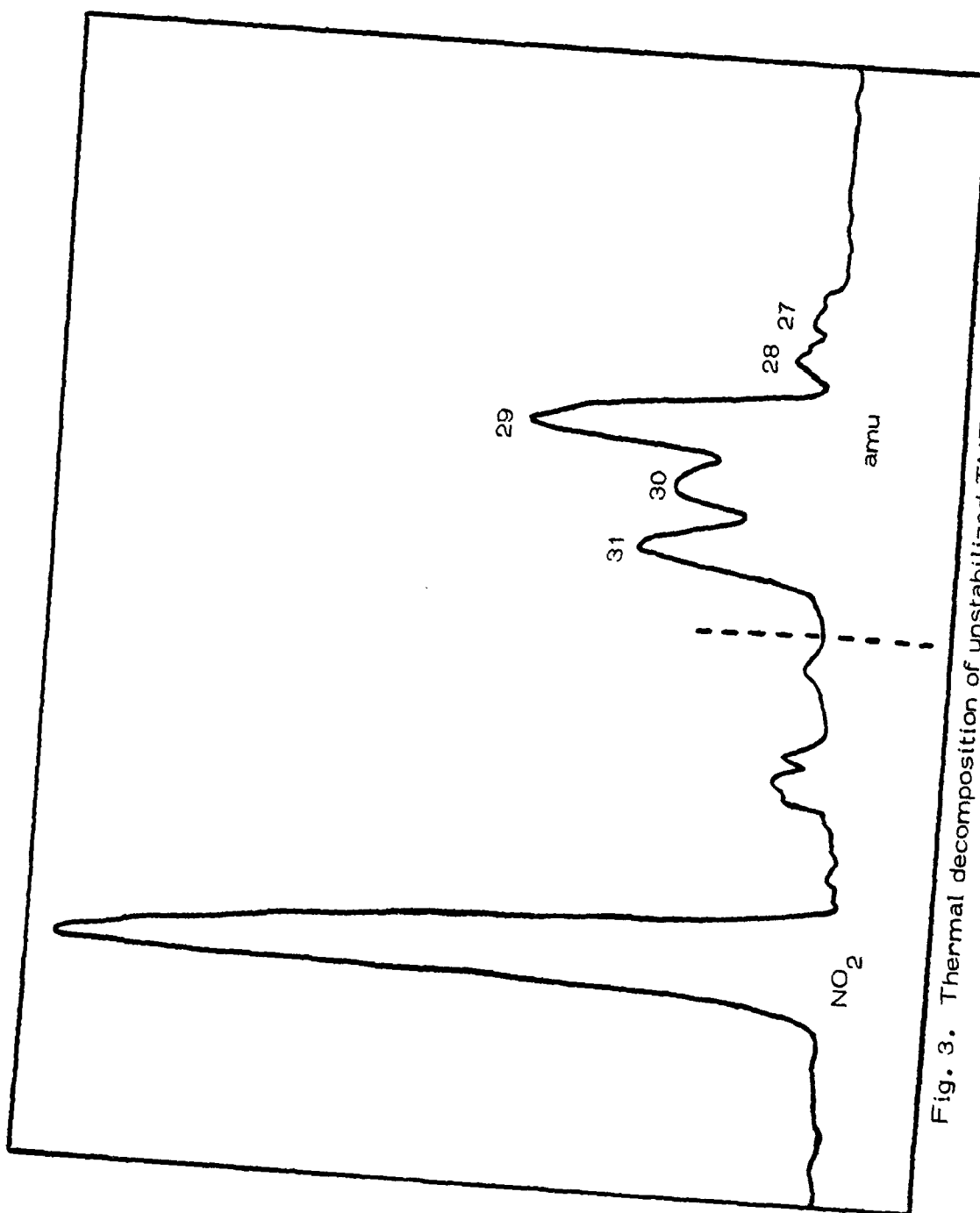


Fig. 3. Thermal decomposition of unstabilized TMETN at 50 C.  
The mass spectra are relative only within the dashed lines.

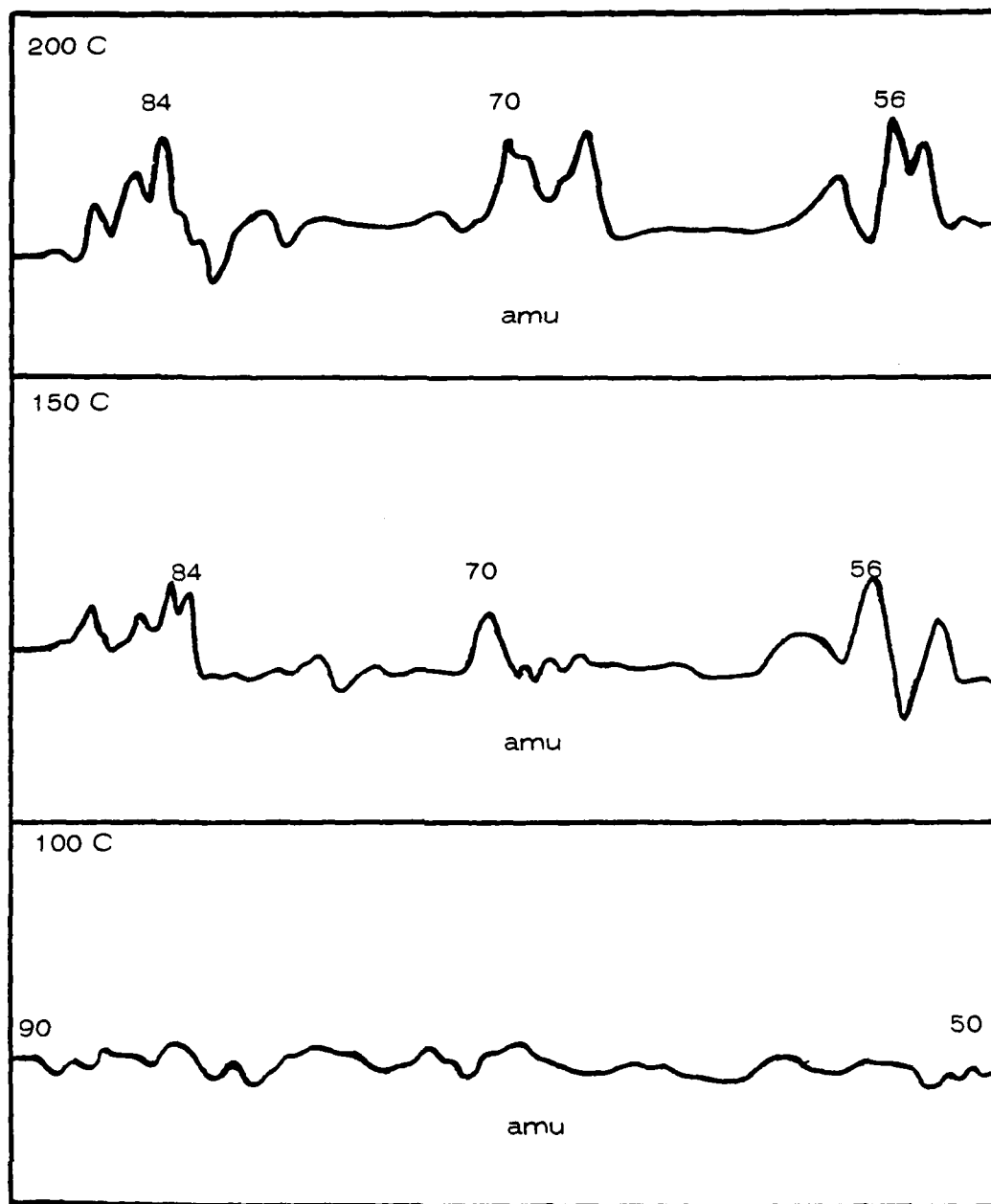


Fig. 4. Thermal decomposition of BEMO at three isothermal temperatures: 100, 150 and 200 C. The mass spectra are in the range 50 - 90 amu.

Above 200 C several prominent high amu peaks appear, indicating that both decomposition and depolymerization are occurring simultaneously. Figure 5 shows the increase in concentration as a function of temperature of several decomposition products. It can be seen that these mass peaks at amu values of 98, 102 and 112 increase rapidly with temperature. An activation energy,  $E_a$ , of  $60 \pm 10$  kcal/mol is calculated within this temperature range (see Fig. 6). This was accomplished by plotting the log of the relative intensities of the 98 atomic mass peaks against the reciprocal of the absolute temperature.

At 230 C the depolymerization of BEMO definitely occurs (Fig. 7), with both higher and lower amu fragments of depolymerization and decomposition. As thermal energy is adsorbed in the polymer the ethoxy methyl groups attached to the central carbon begin to decompose, releasing a number of low molecular weight fragments. The decomposition at this temperature produces many small amu fragments in the range of 13 to 18 amu, including CH, CH<sub>2</sub>, CH<sub>3</sub>, OH and H<sub>2</sub>O (Fig. 8). Numerous fragments are also produced in the 26 to 32 amu range (also shown in Fig. 8). Decomposition products in the 40 to 45 amu range can be seen in the third segment of this figure. The spectra are continuous only within the dashed lines. Figure 9 shows a 100 mass unit scan of BEMO at 260 C. While decomposition is occurring the backbone of the polymer also depolymerizes with multiples of the three-carbon backbone released as vapor species. The relatively low concentration of the monomer probably indicates that although depolymerization of the polymer is occurring, a considerable amount of decomposition is also taking place and that the higher amu species (below and above the monomer) are depolymerized fragments of the backbone where the bonding structure to the ethoxy methyl groups has been destroyed.

The mass spectrometric studies indicated that complex mechanisms were involved. The D.S.C. experiments on BEMO by R. B. Jones of Lehigh University produced thermograms (Fig. 10) showing four finger-like peaks which were attributed to the complex decomposition processes. An Arrhenium plot of the  $\ln k$  vs.  $1/T_D$  yielded an activation energy of 52.4 kcal/mol.

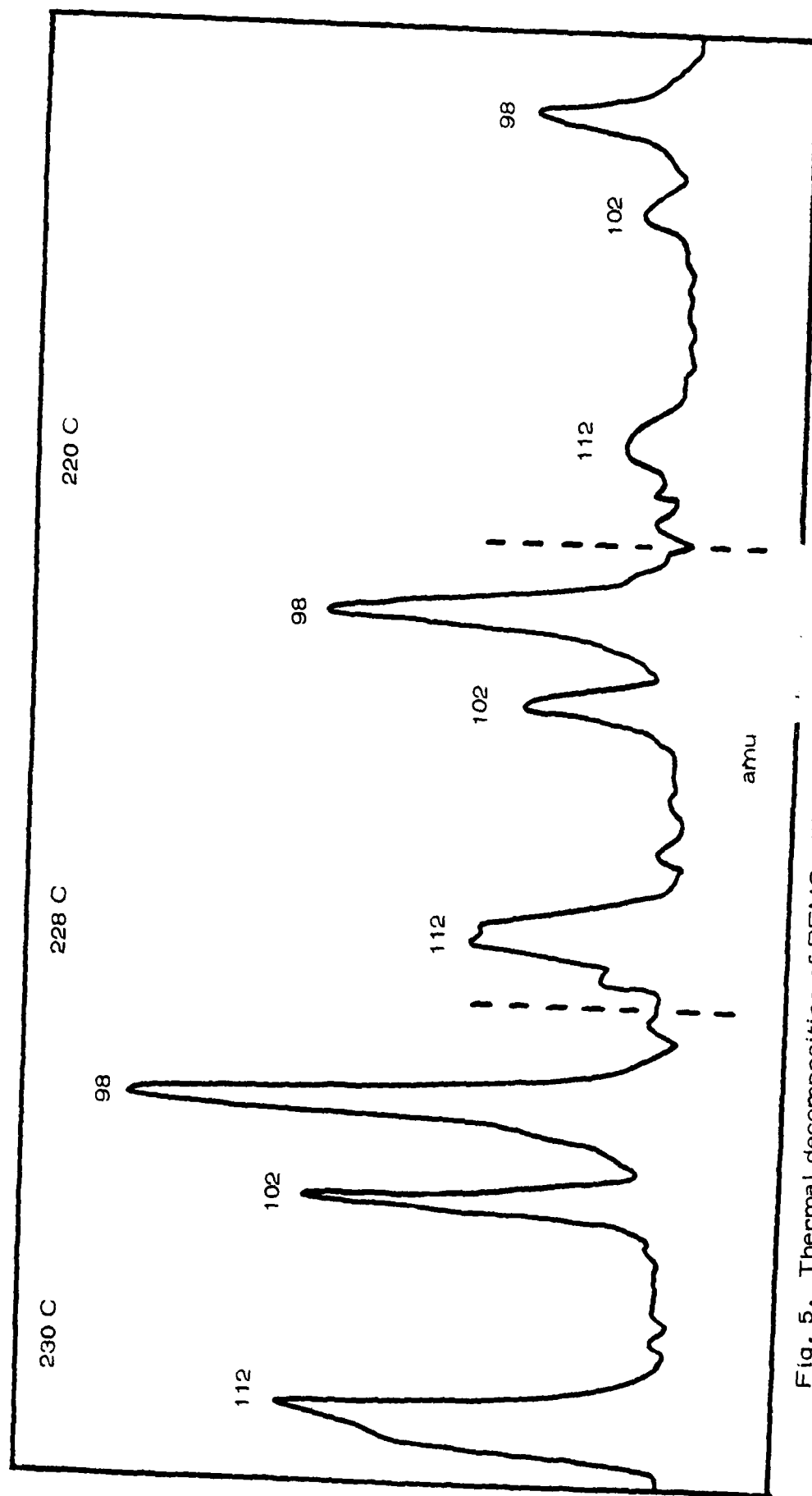


Fig. 5. Thermal decomposition of BMO within the range 220 to 230 C

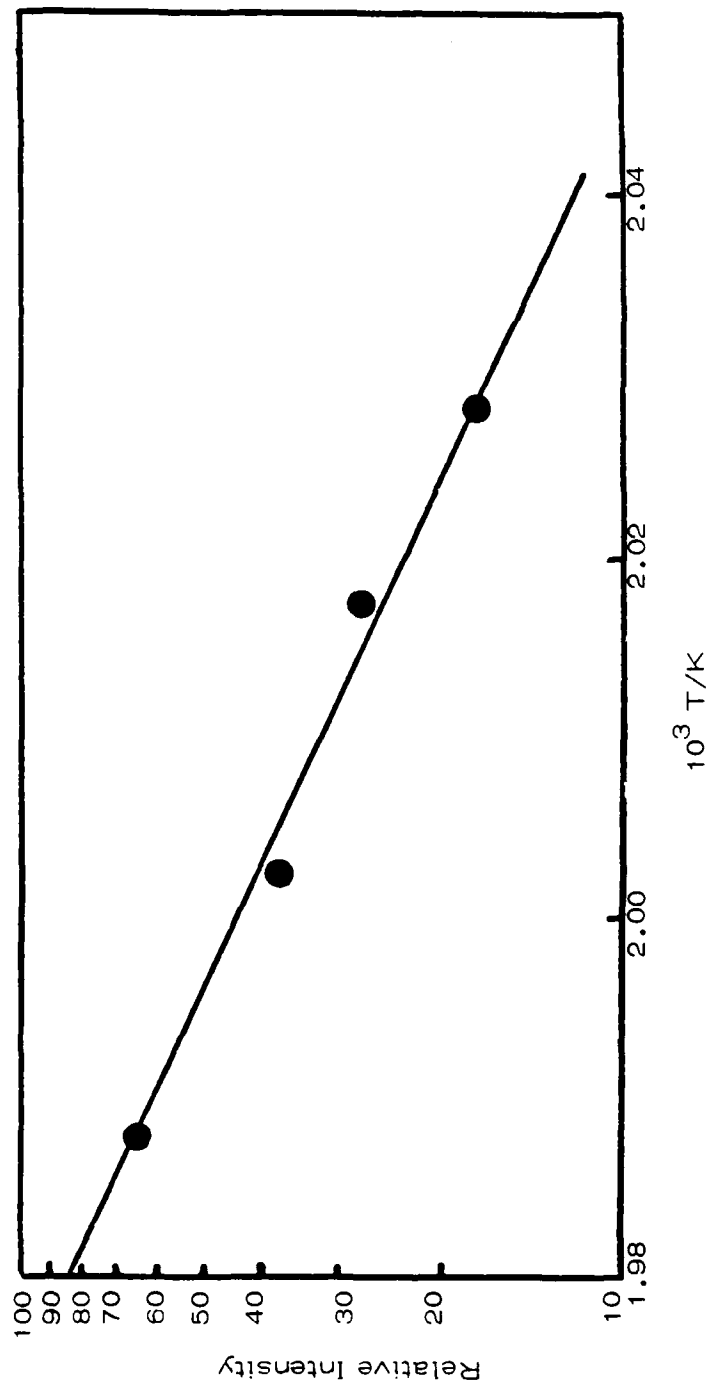


Fig. 6. Plot of the intensity of the 98 amu peak against the reciprocal of the absolute temperature ( $220 - 230^\circ\text{C}$ ), yielding an  $E_a$  of  $60 \pm 10$  kcal/mol

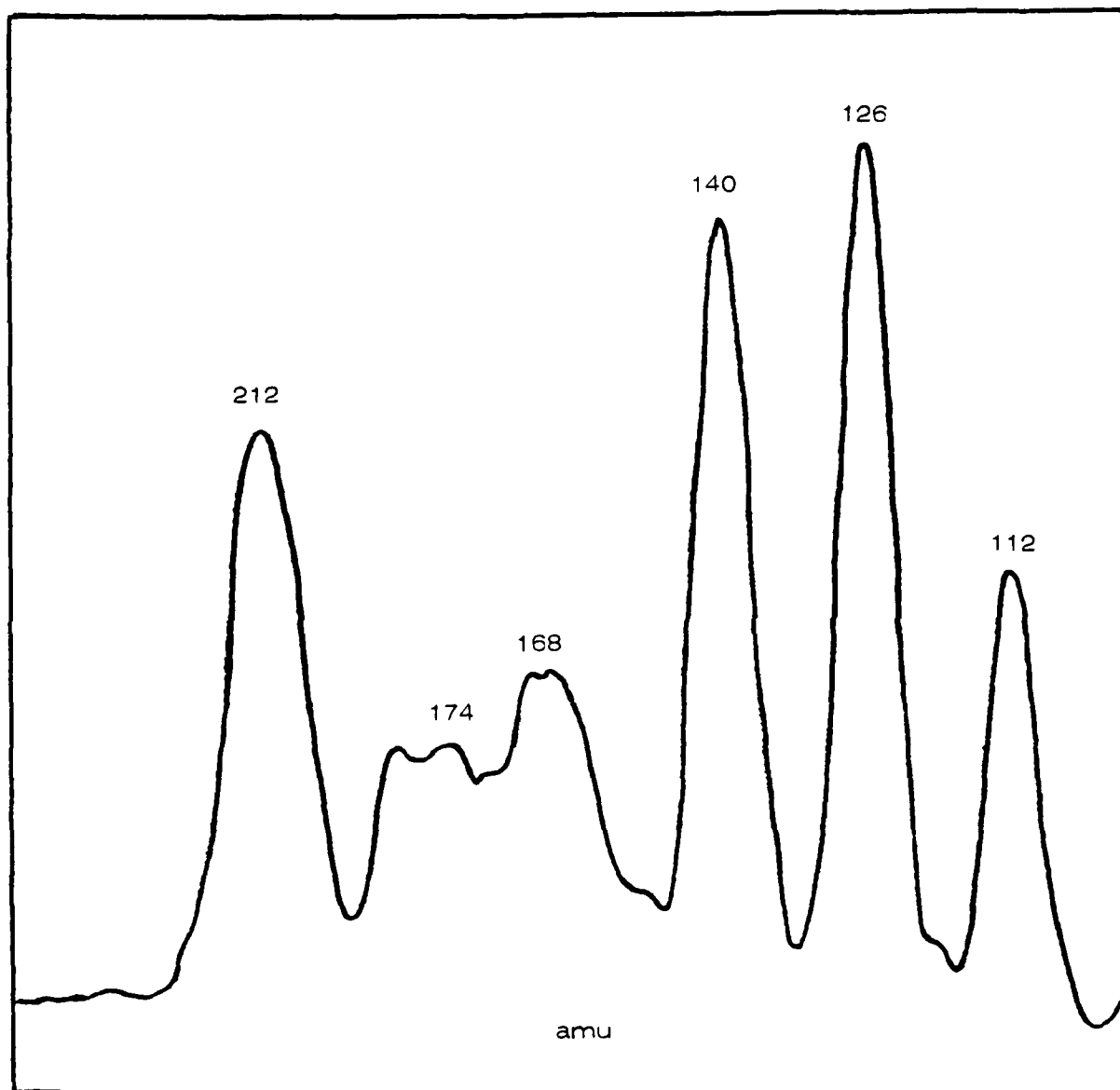


Fig. 7. Decomposition and depolymerization products of BEMO at 230 C

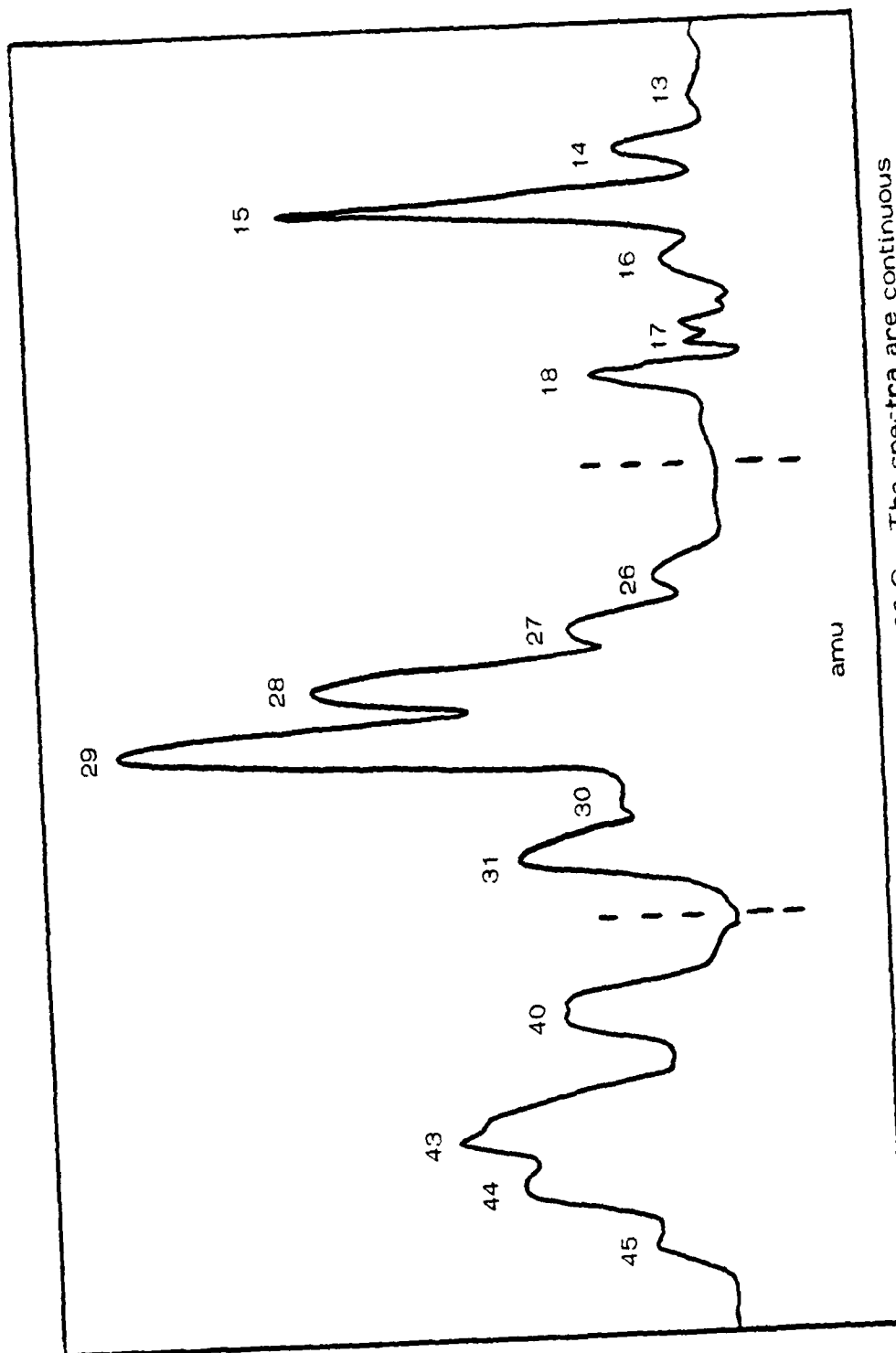


Fig. 8. Decomposition fragments of BEMO at 230 C. The spectra are continuous only within the dashed lines.



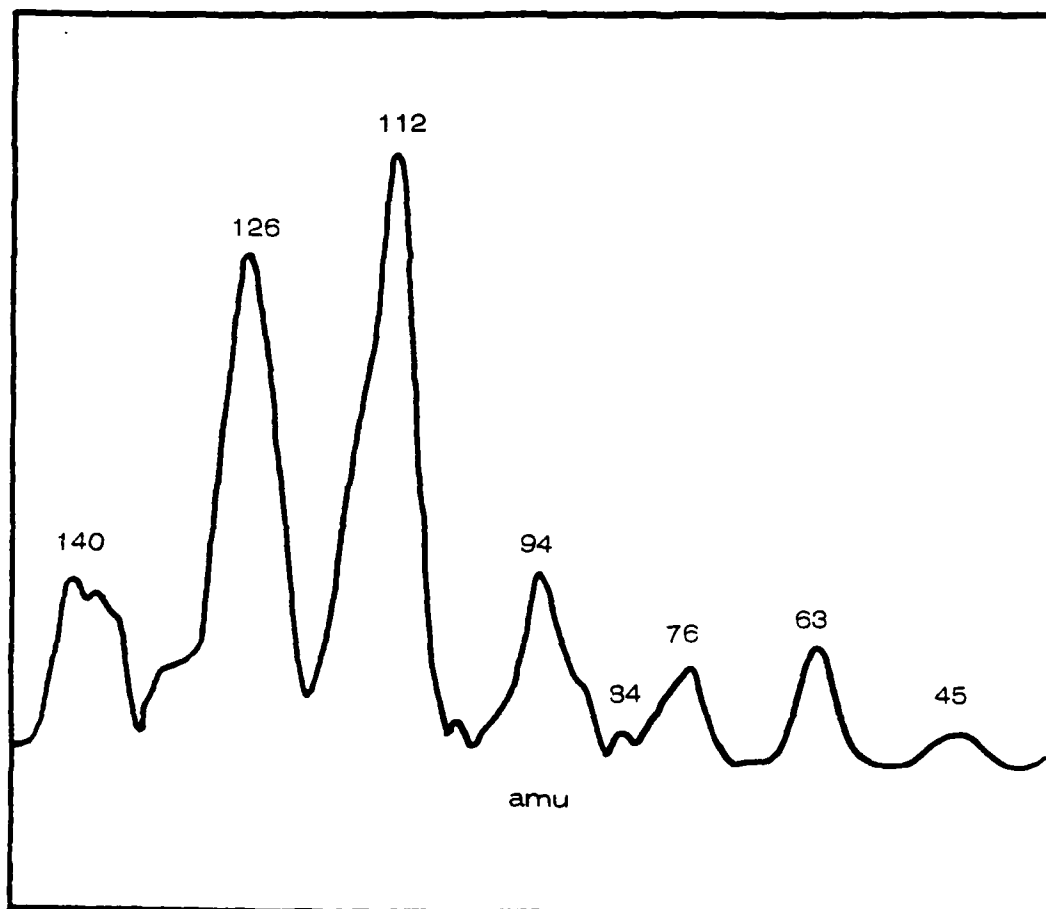


Fig. 9. 100 mass unit scan of BEMO at 260 C

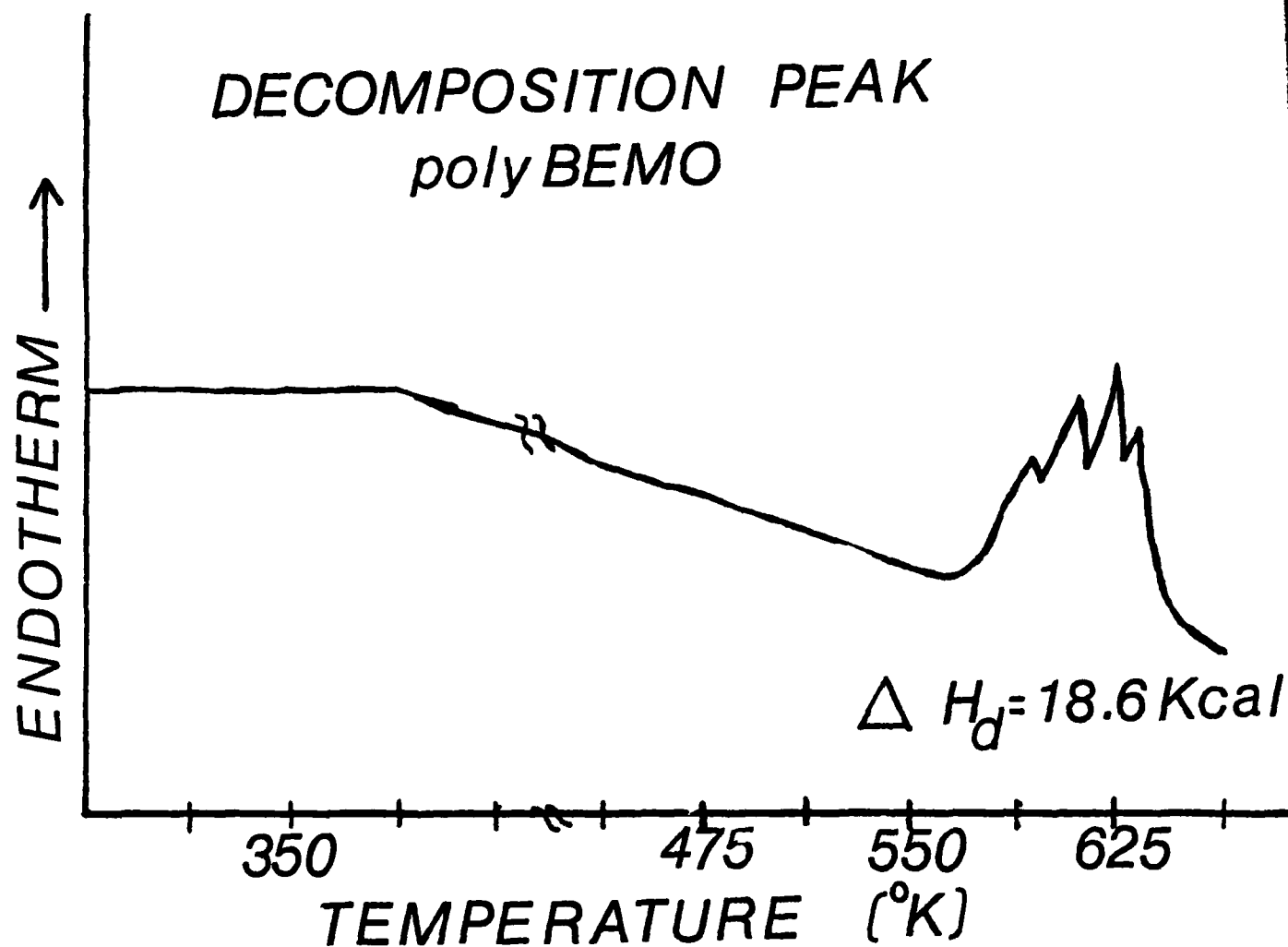
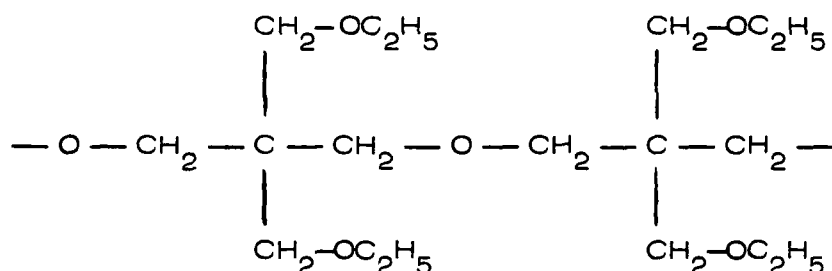


Fig. 10. D.S.C. thermogram of BEMO

From the mass spectra Jones has proposed a mechanism for the decomposition, suggesting that the major route of degradation is through the cleavage of the C-O bond both in the appendages and in the backbone of the chain. This is consistent with the fact that a quaternary carbon-carbon (C-C) bond is stronger than a carbon-oxygen (C-O) bond by about 5 kcal/mol.

Apparently the C-O bond in the side chain breaks first. A possible explanation for this occurrence can be seen from an examination of the dimer:

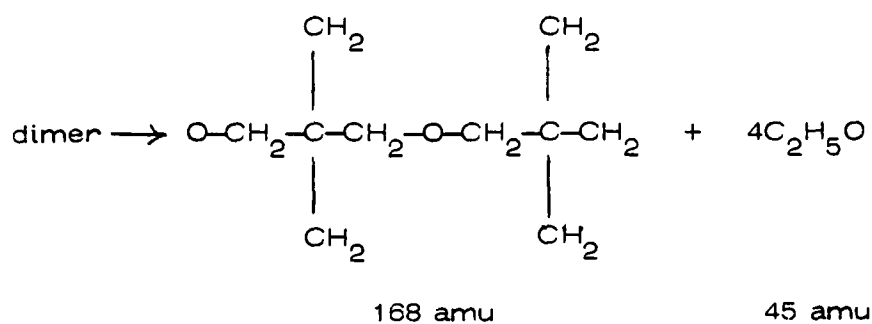


The carbon-oxygen bonds of the backbone are equal in strength due to the symmetric nature of the structure. In the side chain the quaternary carbon-carbon bond is stronger than the C-O bond of the ethoxy methyl group.

Thus it appears that the main mode of cleavage is the C-O bond which is slightly weaker than the quaternary C-C bond. The C-O bond in the appendage breaks before the C-O bond in the main chain since the C-O bonds in the backbone are equal in strength due to the symmetry, while C-O bonds in the appendage are weakened due to the quaternary C-C bond.

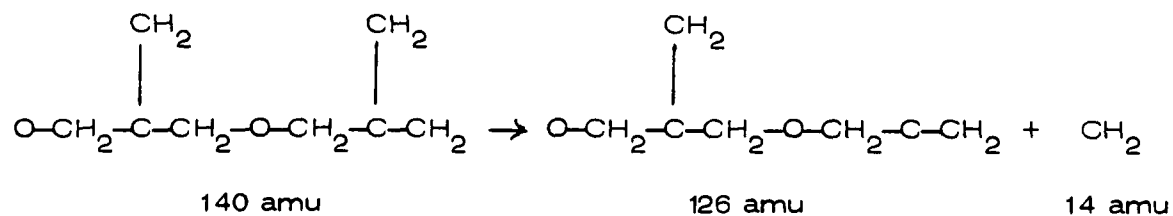
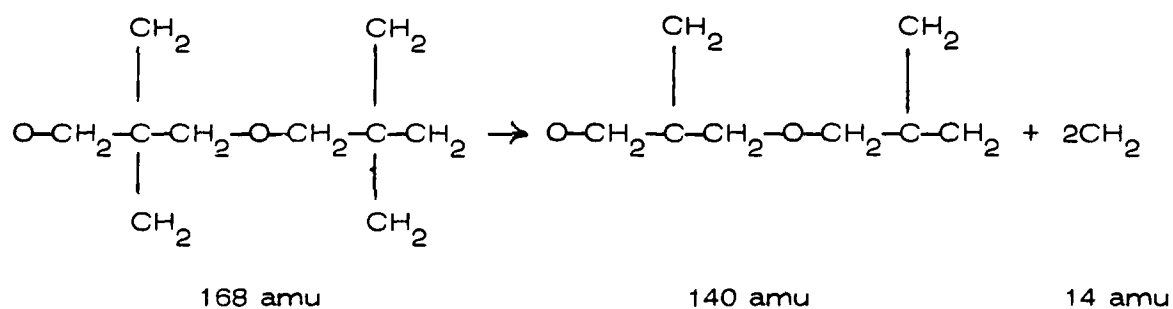
Although the kinetics and mechanisms of BEMO are quite complicated, the clearly defined mass peaks (Fig. 7) suggest a step-wise degradation mechanism as follows:

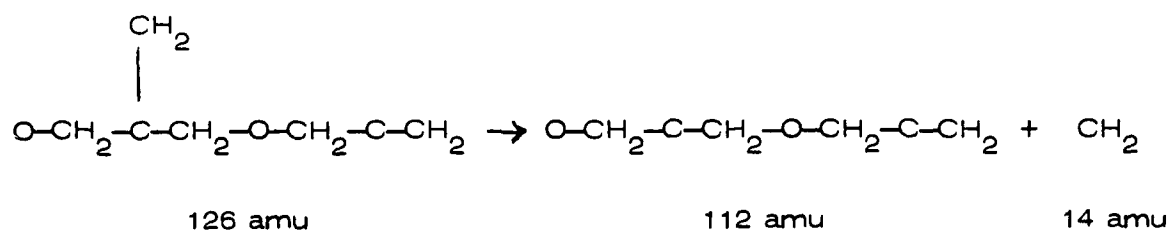
The dimer decomposes from its original 348 amu value to



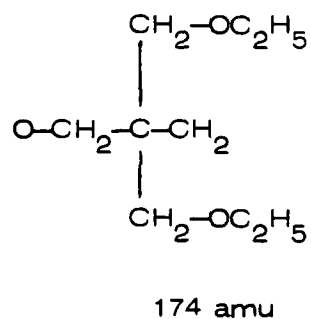
by losing the four ethoxy groups.

The remaining structure continues to lose methylene groups,  $\text{CH}_2$ , as

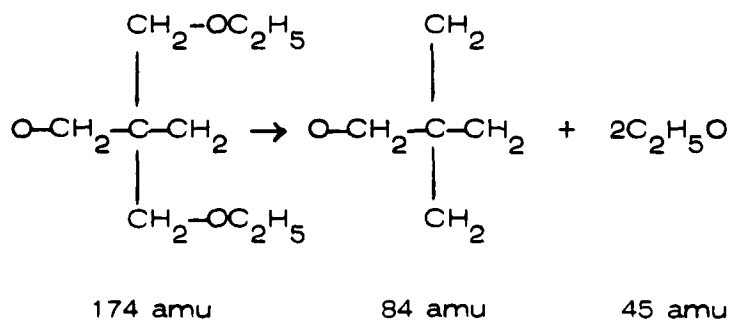




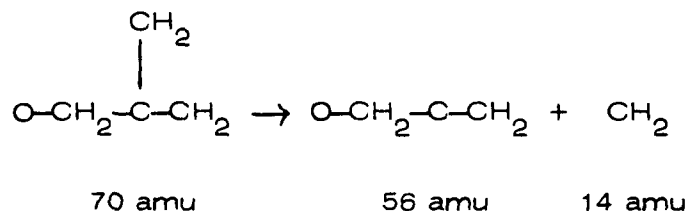
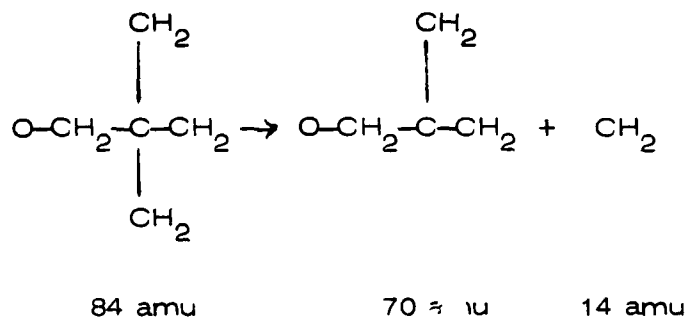
Likewise, the mass spectra of Fig. 4 support the monomeric component



decomposition by also losing the two ethoxy groups:



This is followed by the release of CH<sub>2</sub> groups as



Reactions of the fragments within the effusion cell produce other products as shown in Fig. 8.

## 2. Thermal Decomposition of BFMO

Thermal decomposition experiments were commenced on bis (fluoro methyl) oxetane, BFMO. The polymer was found to have a melting point of  $105 \pm 2$  C. The polymer was found to be quite stable to 200 C. At 225 C HF at amu 20 was observed as a decomposition product. Other decomposition products observed at this temperature included 42, 44, 45, 47, 54, 56 and 60 (Fig. 11).

At temperatures above 250 C depolymerization occurs. Intensity peaks ranging from 75 to 244 amu can be seen in Fig. 12. The

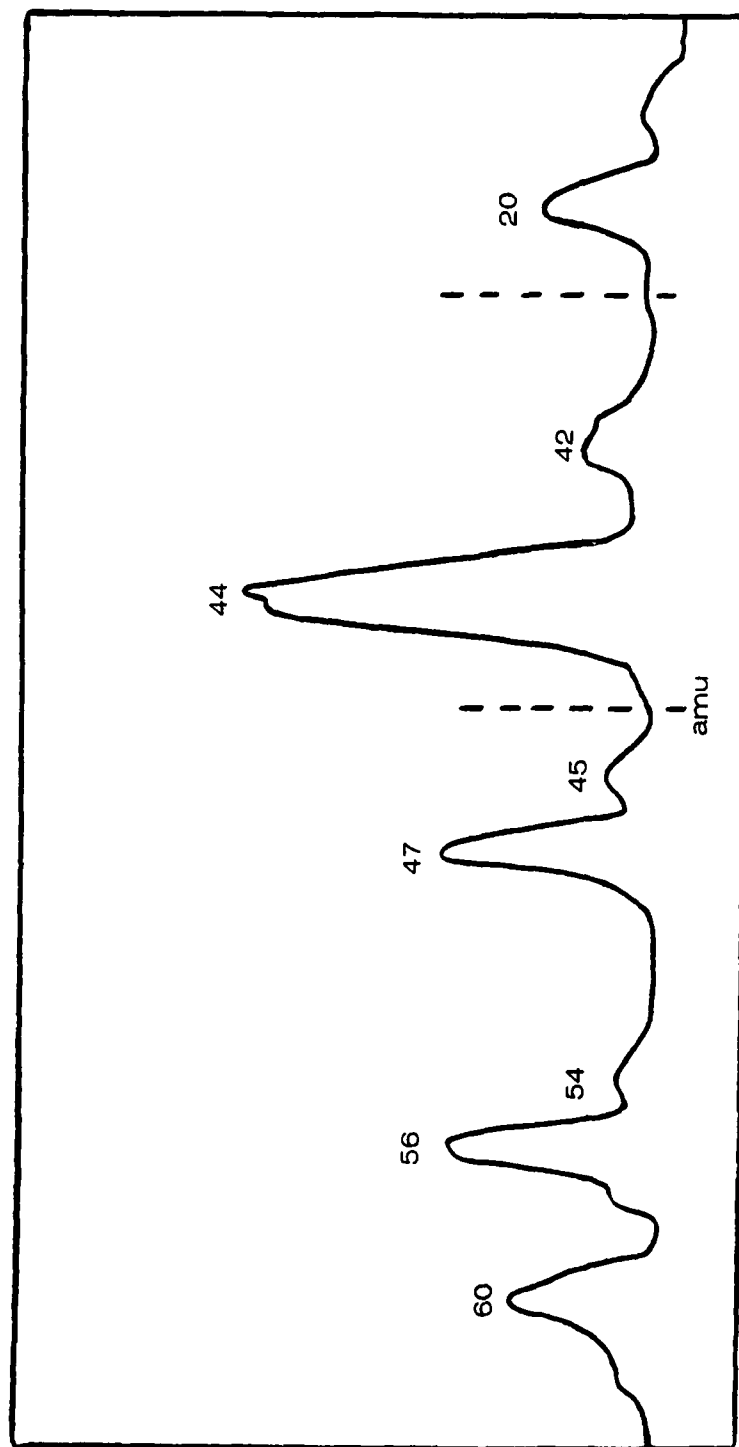


Fig. 11. Decomposition products of BFMO at 225 C in the amu range 20 - 60.  
Intensities are relative only within the dashed lines.

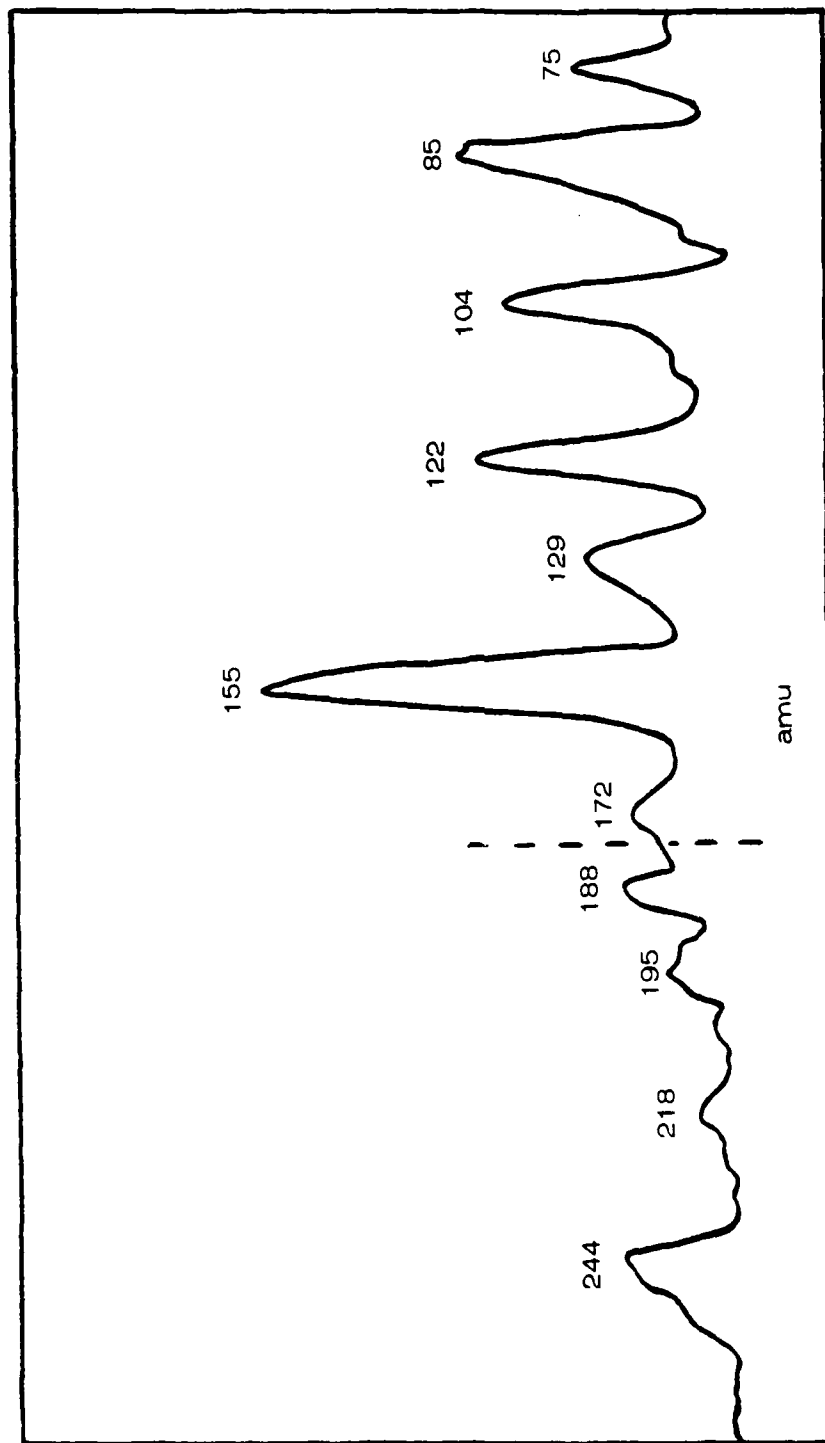


Fig. 12. Depolymerization of BFMO at 255 C. Intensities are relative only within the dashed lines.



molecular weight for the monomer is 122 and 244 for the dimer. Peaks for both of these are shown in Fig. 12, although their concentrations are not relative.

D. Thermal Decomposition of New Nitramines

1. 2,6,tetranitro-4,8,dinitro-4,8,diazo cyclooctane

The investigation of the cyclooctane ring compound obtained from the White Oak Naval Surface Weapons Center was continued. After initial release of two  $\text{NO}_2$  groups at approximately 150 C a stable gaseous cyclooctane ring compound appears at amu 292, with a probable configuration of single  $\text{NO}_2$  groups on the 2,6 C and 4,8 N ring atoms. This configuration appears in the gaseous phase at approximately 300 C (Fig. 13).

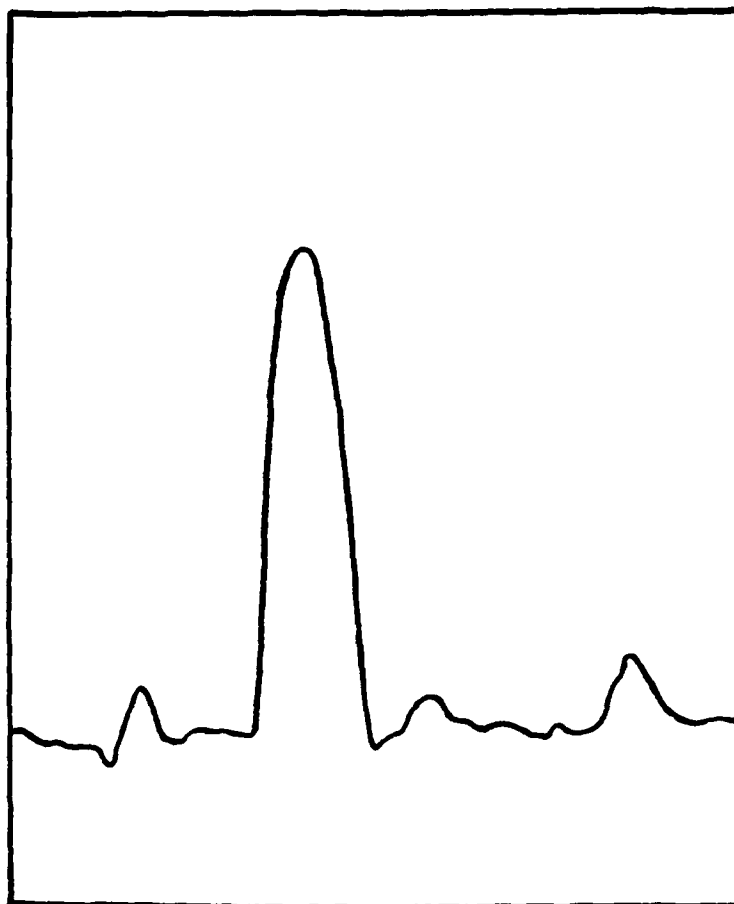


Fig. 13. High temperature stable gaseous species at 280 C resulting from the thermal decomposition of 2,6 tetranitro-4,8 dinitro-4,8 diazo cyclooctane

APPENDIX A

MASS SPECTROMETRIC KINETIC STUDIES ON SEVERAL  
AZIDO POLYMERS

## MASS SPECTROMETRIC KINETIC STUDIES ON SEVERAL AZIDO POLYMERS

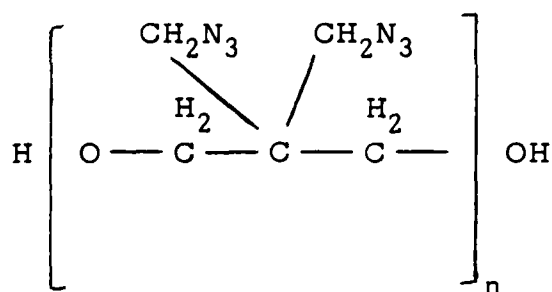
Milton Farber, S. P. Harris and R. D. Srivastava  
Space Sciences, Inc., Monrovia, California

A mass spectrometric study of the thermal decomposition was made on four azido polymers which are possible new candidates for propellant formulations: bis azido methyl oxetane (BAMO), azido methyl methyl oxetane (AMMO), azido oxetane (AZOX), and glycidyl azide polymer (GAP). All the polymers begin to decompose at approximately 120 C, with the primary decomposition mechanism being the rupture of the azide bond to release molecular nitrogen. Activation energies obtained were 42.7 kcal/mole for BAMO, 43.6 kcal/mole for AMMO, 40.1 kcal/mole for AZOX, and 42.2 kcal/mole for GAP. The polymeric  $E_a$  values were close to those of a number of azido monomers having  $E_a$  values of 39 to 40 kcal/mole. Secondary decomposition at higher temperatures (above 200 C) involved rupture of the carbon backbone into smaller fragments. Irradiation at 366 nm (3.29 eV) ruptured the azide bonding with considerable cross-linking, transforming the polymer from a viscous liquid into a rubbery material.

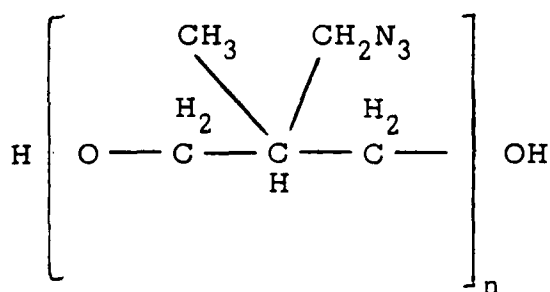
## INTRODUCTION

In the search for new energetic binder materials a great deal of interest has centered recently on one group of azido compounds in particular. These current prime candidates for propellant formulations include four polymeric materials, three of which have a repeating three-carbon backbone and one of which has a repeating two-carbon backbone, with one or two azide groups attached directly or indirectly. Their molecular weights range from 2000 to 5000 molecular mass units. These polymeric compounds are:

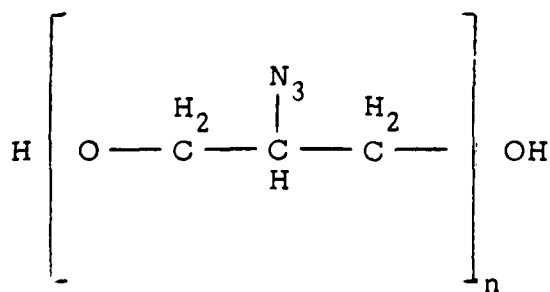
bis azido methyl oxetane (BAMO),



azido methyl methyl oxetane (AMMO),

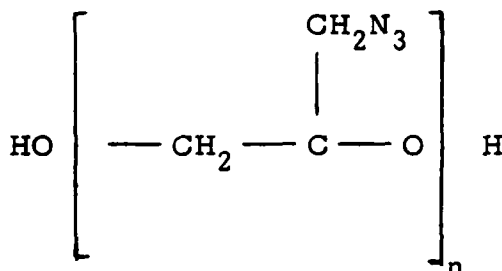


azido oxetane (AZOX),



and

glycidyl azide polymer (GAP)



The thermal decomposition study of these four polymers was undertaken with the aid of effusion-mass spectrometry to determine primary and secondary decomposition mechanisms, activation energies and products of decomposition. Their stability to UV radiation under ambient conditions was also investigated.

A search of the open literature revealed no prior publications involving the four polymers covered in this paper.

#### EXPERIMENTAL APPARATUS AND PROCEDURES

Details of the dual vacuum chamber-quadrupole mass spectrometer system used in these experiments have been presented previously (1), as well as a schematic depiction of the apparatus (2). The polymer samples, weighing 5 to 50 mg, were placed in a small pyrex capsule within an alumina effusion cell 25 mm long with an inside diameter of 6.8 mm; an elongated orifice 0.75 mm in diameter by 5.5 mm long was employed for beam collimation (see Fig. 1). The temperature was measured with the thermocouple in contact with the sample and was accurate to  $\pm 2^\circ\text{C}$  at the absolute temperature and within  $\pm 0.5^\circ\text{C}$  as a differential temperature. The cell was positioned within 5 cm of the ionization chamber of the mass spectrometer, allowing species leaving the solid or liquid surface to be measured within approximately 10  $\mu\text{sec}$  after their exit from the cell. These times are calculated from species velocities effusing from the effusion cell and will vary with cell temperature and pressure. The alumina cell was heated

by a resistance furnace and temperature measurements were made by means of thermocouples imbedded in the cell body. The method for determining ion intensities, mass spectrometer resolution, as well as the measurement of the isotopic abundance ratios, has been presented previously (3). All quadrupole experimental mass discrimination effects were taken into account and the necessary corrections to ion intensity relationships were made when quantitative partial pressures were desired. Only the chopped, or shutterable, portion of the intensities was recorded, since the mass spectrometer was equipped with a beam modulator and a phase sensitive amplifier. The experimental procedure has been described previously (1,3-7).  $^{127}\text{I}$  and  $^{254}\text{I}_2$  as well as the standard gases  $\text{N}_2$ ,  $\text{O}_2$ ,  $\text{NO}_2$ ,  $\text{NO}$ ,  $\text{H}_2$ , and  $\text{NH}_3$  were employed for the amu calibration. Partial pressures were obtained from the calibrated data by means of the relationship

$$p_i = \frac{I_i (\sigma \gamma)_a}{I_a (\sigma \gamma)_i} p_a,$$

where a is the calibrated species, i is the unknown species, and  $\sigma$  and  $\gamma$  are, respectively, ionization cross sections and electron multiplier corrections.

It was necessary to ascertain with a high degree of confidence that the measured ion intensities were those from the parent species and not from the fragments of the larger molecules. In order to ensure the survival of ions from the parent species the mass spectrometer was operated at low ionization voltages (i.e., 1 to 2 volts above appearance potentials (1,3-9) when establishing a species identification. For example, the ionization potential of CO is 14 eV whereas the IP for  $\text{N}_2$  is 15.6 eV. Thus the concentration of species at amu 28 at an electron impact energy of  $< 15.5$  volts would be entirely due to CO.

Melting points were obtained only for BAMO since the other three polymers are viscous liquids at ambient temperatures. Decomposition rates to determine activation energies were obtained at constant electron impact ionization voltages of 20 eV and at a heating rate of one degree per minute.

The experiments involving UV radiation employed 254 nm and 366 nm wavelengths, corresponding to 4.88 eV and 3.39 eV, respectively. These energies correspond to 112 kcal/mole and 78 kcal/mole, respectively. The deposition energy 2.5 cm from the lamp is 7200  $\mu\text{watts}/\text{cm}^2$  and 10,000  $\mu\text{watts}/\text{cm}^2$  for the short and long wave lamps. The samples weighed 25 mg and were spread over a 1 sq cm area.

## RESULTS AND DISCUSSION

### Weight Loss and Effusion Mass Spectrometer Experiments

#### Thermal decomposition of bis azido methyl oxetane (BAMO)

Isothermal experiments were performed at  $10^{-7}$  torr from 80 to 250 C on BAMO polymer with a molecular weight of approximately 3000.

Weight loss experiments on 25 mg samples of BAMO were performed for periods of 3 hours each at temperatures of 82, 100, 118, 130, 135, and 202 C. These data are presented in Table 1. No apparent decomposition occurred at 80, 100, or 120 C, although at 120 C the sample turned from white to a slightly off-white, or cream, color. Effusion cell pressures were determined by the Knudsen equation,

$$p_{\text{mm}} = 17.4 \frac{G}{KA} \sqrt{\frac{T}{M}}$$

where  $G$  = weight loss in  $\text{g sec}^{-1}$

$K$  = Clausian factor

$A$  = orifice area in sq cm

$T$  = temperature in degrees K

$M$  = molecular weight

Slight decomposition began at 130 C, with a rate of decomposition at 200 C almost 20 times that at 130 C. A 25 mg sample maintained at 200 C for 3 hours lost 80% of its initial mass, leaving behind a carbonaceous tar residue. The melting point of the BAMO polymer was found to be 75 C.

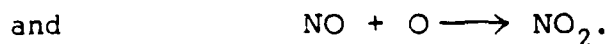
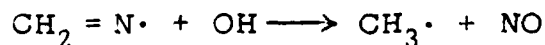
Employing the sample container shown in Fig. 1, effusion-mass spectrometer experiments were performed on 25 mg BAMO samples. These spectra were obtained at an ionization voltage of 20 eV. The release of



molecular nitrogen is observed as low as 130 C; a much higher rate of N<sub>2</sub> evolution occurs at temperatures above 160 C, as can be seen in Fig. 2, which depicts the N<sub>2</sub> concentration as a function of temperature. At any given temperature the decomposition rate is essentially constant, whether in a heating or cooling cycle.

An activation energy study of the primary decomposition path, the release of N<sub>2</sub> from the azide groups, was also completed. The heating rate for the temperature dependence investigation was 1° per minute. A plot of the N<sub>2</sub> intensity versus the reciprocal of the absolute temperature yielded an E<sub>a</sub> for the BAMO polymer of 178.7 kJ mol<sup>-1</sup> (42.7 kcal/mole) (see Table 2). This study shows that the primary mechanism for BAMO decomposition is the release of N<sub>2</sub> from the rupture of the azido bond. The three-carbon backbone of the polymer appears to remain intact initially since other gaseous species are not observed until the sample is heated to higher temperatures, approximately 160 C.

In addition to molecular N<sub>2</sub>, the mass spectrometer showed a peak at 27 amu corresponding to HCN as well as peaks of amu 2, 14, 15, 16, 17, and 18 attributable to H<sub>2</sub>, CH<sub>2</sub>, CH<sub>3</sub>, O (fragment of O<sub>2</sub>), OH and H<sub>2</sub>O, respectively. A representative spectrum of this secondary decomposition at 200 C is shown in Fig. 3. The intensities in Fig. 3 are only relative within the dashed lines. The products in the 40 to 48 amu range are presumably due to effusion cell reactions. The formation of NO<sub>2</sub>, for example, may require cell reactions of the following type:



High temperature (200 C) decomposition products of BAMO include mass peaks at 40, 42, 43 and 44 amu. Within the effusion cell, where numerous collisions between gaseous species and the cell walls and also with the condensed polymeric materials can occur, the probability is high that some of the products observed mass spectroscopically are produced within the effusion cell itself and are not original decomposition products

from the condensed phase. The three-membered carbon backbone of BAMO is definitely disintegrating at 200 C, as can be seen in Fig. 3, with the production of HCN at amu 27 and CH<sub>2</sub>O and CH<sub>2</sub>OH at amu values of 30 and 31. The relative concentrations of these species, however, are low compared with the combined N<sub>2</sub> + CO evolution.

#### Thermal decomposition of azido methyl methyl oxetane (AMMO)

The thermal decomposition of a relatively new azide polymer, azido methyl methyl oxetane (AMMO) was also investigated. This polymer is similar to BAMO except that it has one azido methyl group on the center carbon of the three-carbon backbone, whereas BAMO has two.

AMMO was found to have a somewhat higher stability than the other azide polymers. A study of N<sub>2</sub> evolution, which is the onset of thermal decomposition, shows that it continues until the destruction of the azide group is completed when no further release of molecular N<sub>2</sub> is observed. An activation energy of 182.4 kJ mol<sup>-1</sup> (43.6 kcal/mole) was calculated from these data (Table 2).

The thermal decomposition of AMMO was measured from 120 to 300 C. Its stability can be seen in Fig. 4, which shows very little backbone decomposition at 210 C. At 290 C a 30 amu peak corresponding to CH<sub>2</sub>O indicates backbone decomposition (Fig. 5). The relative OH and H<sub>2</sub>O concentrations increase significantly at 290 C. Also some methyl radicals at amu 15 were observed.

A qualitative indication of the relative thermal stability of BAMO and AMMO at 235 C can be seen in Fig. 6.a. Considerably more H<sub>2</sub>O is apparent from BAMO decomposition (Part B, Fig. 6.a.), indicating the release of greater quantities of OH, which recombine within the effusion cell to form water. Also, the relative amount of CH<sub>3</sub> radicals is larger from BAMO decomposition than from that of AMMO. As the temperature increased from 215 to 235 C (Fig. 6.b.) the thermal decomposition rate of BAMO increased rapidly, creating a fairly high cell pressure causing OH recombination to form H<sub>2</sub>O. This did not occur with AMMO; even at temperatures as high as 290 C the OH/H<sub>2</sub>O ratio of AMMO appeared fairly constant.

#### Thermal decomposition of azido oxetane (AZOX)

An azido polymer, AZOX, in which the azide group is directly attached to the backbone central carbon was studied. As in the previous azido polymers, molecular  $N_2$  was the first thermal decomposition product occurring at approximately 120 C. By plotting the log of the  $N_2$  intensity against the reciprocal of the absolute temperature an activation energy of  $167.8 \text{ kJ mol}^{-1}$  (40.1 kcal/mole) was obtained (Table 2). As the temperature is raised above 200 C the three-membered carbon backbone of AZOX begins to disintegrate more rapidly with the ion spectra showing the species  $CH_2$ ,  $CH_3$ , OH, and  $H_2O$  in the low mass range. The higher amu range shows peaks attributed to CO,  $CH_2OH$ ,  $C_2OH$ , and  $CO_2$  at 230 C (Fig. 7). A small ion intensity may be attributed to  $HN_3$  at amu 43; however, it is more likely due to  $C_2H_3O$ .

#### Thermal decomposition of glycidyl azide polymer (GAP)

The three polymers, BAMO, AMMO and AZOX had their azide groups attached directly or indirectly to the central carbon of the three-membered polymeric oxetane backbone. A fourth azido polymer investigated was the glycidyl azide polymer, with a repeating two-carbon backbone.

As in the case of the other azido polymers, the GAP appears to be fairly stable to 120 C, when molecular  $N_2$  is released. The results of the decomposition study of this polymer as a function of temperature were employed to obtain an activation energy for the primary decomposition mechanism, the release of  $N_2$ . For a 20-degree rise in temperature the rate of  $N_2$  evolution increased by approximately a factor of 10. In the amu range 24 to 32 the major ion intensity constituent is molecular  $N_2$ . This appears to be the same pattern as found in the thermal decomposition of BAMO. A plot of the log  $N_2$  against  $1/T$ , as shown in Fig. 8, yielded an activation energy of  $176.6 \text{ kJ mol}^{-1}$  (42.2 kcal/mole). However, at temperatures above 170 C a slight intensity of amu 27, HCN, was observed, approximately 1% to 2% of the  $N_2$  intensity. It is likely that secondary decomposition begins at a slightly lower temperature for GAP than for BAMO. An example of the decomposition products in the 14 - 48 amu range at 200 C can be seen in Fig. 9. We understand that work has been performed to obtain thermal decomposition kinetics of GAP (10) and that the measured activation agrees with the value reported here.

### Azido Monomers

Although not directly involved in energetic binder formulations, it was felt that the thermal decomposition of a representative azido monomer should be obtained. The AZOX monomer was chosen for this study, with its vapor released directly into the heated effusion cell.

Figure 10 shows the mass spectra of the thermal decomposition from 160 to 195 C. In this 35-degree range the  $N_2$  intensity increased by a factor of 20. These graphs are composites of the individual peak heights and are continuous within the dashed lines as a function of temperature. In this temperature range for the AZOX monomer an activation energy of 40 kcal/mole was obtained. This apparently is typical of azide monomers, as shown in a recent publication by Isayev, et al (11). Several monomers were investigated, with reported  $E_a$  values of approximately 39 kcal/mole (Table 2) for aliphatic azides including  $\beta$ -triazoethanol, 1,3,diazide propanol, 1,3,diazide propylene ester of acetic acid, and 1,3,diazide propylene acid.

### Effects of UV Radiation

The azido polymers were subjected to UV radiation as described in the Experimental Section. After several preliminary experiments at 254 nm tests were discontinued due to considerable adsorption by air (12). Short wave UV irradiation studies would thus best be accomplished in a vacuum enclosure. A typical result, qualitative only, is shown in Fig. 11 for AMMO. Employing 360 nm light the samples were irradiated at distances of 2.5 cm ( $10,000 \mu\text{watts}/\text{cm}^2$ ), 7.5 cm ( $1,120 \mu\text{watts}/\text{cm}^2$ ), and 15 cm ( $380 \mu\text{watts}/\text{cm}^2$ ) for periods up to five hours. The radiation intensity, for example, at a distance of 2.5 cm from the sample surface provided  $36 \text{ J}/\text{cm}^2$  for each hour of exposure. At this wave length the radiation energy is 3.39 eV (78 kcal/mole) which is sufficient to rupture the azide bond and release molecular  $N_2$ . Considerable bubbling appears in the sample, indicating gaseous release. Cross linking apparently takes place, producing rubbery solids from the initial viscous liquids. The irradiated samples (homopolymers and copolymers) were maintained for a number of weeks under ordinary atmospheric conditions as well as under vacuum. No further reactions were observed.

## CONCLUSIONS

All the azido polymers, including their monomers, homopolymers, and copolymers, were found to have activation energies from 165 to 182 kJ mol<sup>-1</sup> (40 to 43 kcal/mole). These results, based on the number of azide materials investigated, should be conclusive evidence that the polymers, copolymers, or monomers decompose primarily by the fracturing of the azide bond. Polymerization apparently has little or no effect on the thermal decomposition of the azide compounds.

The primary mechanism for thermal decomposition of the azido polymer is the fracturing of the azide,  $-N=N_2$ , with the release of molecular  $N_2$ . The kinetics are comparable for all the materials. Once the azide structure is destroyed, in all probability there occurs electron shifting of the unpaired electron from the azide group. Internal electron resonance occurs, which reduces the stability of the remaining organic structure.

Upon continued heating enough thermal energy is adsorbed so that the molecular structure of the polymer undergoes further rupturing of the aliphatic organic bonds with the release of various low molecular weight molecules and radicals. As found in this investigation, the backbone of the AZOX polymer ruptures at lower temperatures than do the BAMO and AMMO polymers. Since the AZOX backbone is immediately affected when the azide group ruptures, its stability is impaired. Thus less thermal energy is required for its decomposition than for the polymers in which the azide group is attached to the methyl group arms. The slightly higher stability of AMMO to BAMO is due to the fact that only one azide group is attached to the arms whereas BAMO has two.

## ACKNOWLEDGMENT

This research was sponsored by the Office of Naval Research, Mechanics Division, under the direction of Dr. Richard S. Miller. Samples of the BAMO, AZOX and AMMO polymers were synthesized and furnished by Dr. G. E. Manser, formerly with SRI International, now with Morton Thiokol Wasatch Division (13). G samples were furnished by Dr. B. Goshgarian of AFRPL and synthesized by Dr. M. B. Frankel of Rockwell International Rocketdyne Division (14). Dr. Kurt Baum of Fluorochem, Inc. supplied the AZOX monomer sample.

# REFERENCES

1. Farber, M., Frisch, M. A. and Ko, H. C., Trans. Faraday Soc. 65, 3202 (1969).
2. Farber, M. and Srivastava, R. D., Combust. Flame 42, 165 (1981).
3. Farber, M. and Srivastava, R. D., Combust. Flame 20, 33 (1973).
4. Farber, M., Srivastava, R. D. and Uy, O. M., J. Chem. Soc. Faraday Trans. I 68, 249 (1972).
5. Farber, M. and Srivastava, R. D., J. Chem. Soc. Faraday Trans. I 70, 1581 (1974).
6. Farber, M. and Srivastava, R. D., J. Chem. Soc. Faraday Trans. I 73, 1692 (1977).
7. Farber, M. and Srivastava, R. D., Chem. Phys. Letts. 51, 307 (1977).
8. Farber, M., Srivastava, R. D. and Moyer, J. M., J. Chem. Therm. 14, 1103 (1982).
9. Farber, M. and Srivastava, R. D., J. Chem. Phys. 74, 2160 (1981).
10. Goshgarian, B., AFRPL, Edwards, California, private communication.
11. Isayev, B. M., Kanashin, S. P., Kozhukh, M. S. and Tokarev, N. P. "Investigation of the Combustion of Certain Organic Azides," Khimicheskaya fizika protessov goreniya i vzryva. Kinetika khimicheskikh reaktsiy. Chernogovka, 1980, 97-101. (Series Note: Vsesoyuznyy simpozium po goreniyu i vzryvu, 6-th Alma-Ata, 23-26 Sept. 1980. Materialy.)
12. Herzberg, G., "Molecular Spectra and Molecular Structure. I. Spectra of Diatomic Molecules," D. van Nostrand, New York 1950.
13. Manser, G. E., "Synthesis of Energetic Polymers," Final Report, Contract N00014-79-C-0525, SRI International, Sept. 1982; Manser, G. E., U. S. Patent No. 4,393,199, July 1983.
14. Frankel, M. B., "Energetic Azide Compounds," Annual Report, Contract N00014-79-C-0043, Rockwell International Rocketdyne Division, March 1980.

Table 1

## Thermal Decomposition of BAMO

Temp. (°C)	Experiment Duration (hours)	Initial Sample Weight (gms)	Final Sample Weight (gms)	Rate of Decomposition (g/sec)	Appearance
82	3	0.0226	0.0226	0	No color change; sample melted
100	3	0.0226	0.0226	0	No color change; sample melted
118	3	0.0226	0.0226	0	Slightly off-white
130	3	0.0248	0.0235	$1.2 \times 10^{-7}$	Cream colored
135	3	0.0347	0.0309	$3.5 \times 10^{-7}$	Cream colored
202	3	0.0252	0.0045	$19.1 \times 10^{-7}$	Brownish-black char

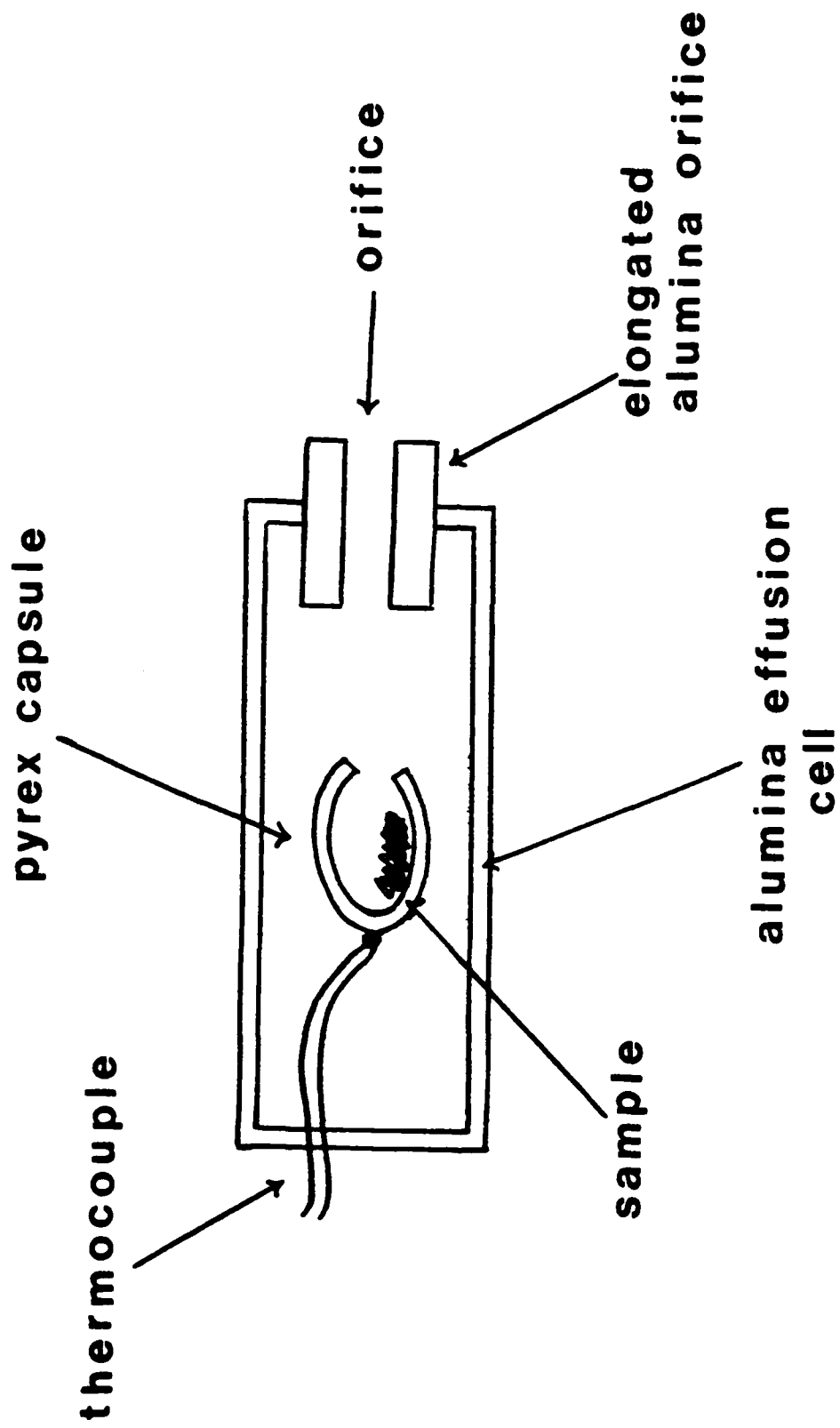


Fig. 1. Sample capsule within effusion cell with elongated orifice



Table 2  
Activation Energies for Azido Polymers and Monomers

		$E_a$	
		<u>kcal mol<sup>-1</sup></u>	<u>kJ mol<sup>-1</sup></u>
<u>Azido Polymers</u>			
BAMO	bis azido methyl oxetane	42.7	178.7
AMMO	azido methyl methyl oxetane	43.6	182.4
AZOX	azido oxetane	40.1	167.8
GAP	glycidyl azide polymer	42.2	176.6
<u>Azido Monomers</u>			
AZOX		40.0	167.4
<i>S</i> -triazoethanol		37.8	158.2 (Ref. 11)
1,3,diazide propanol		38.2	159.8 (Ref. 11)
1,3,diazide propylene ester of acetic acid		38.8	162.3 (Ref. 11)
1,3,diazide propylene acid		38.8	162.3 (Ref. 11)

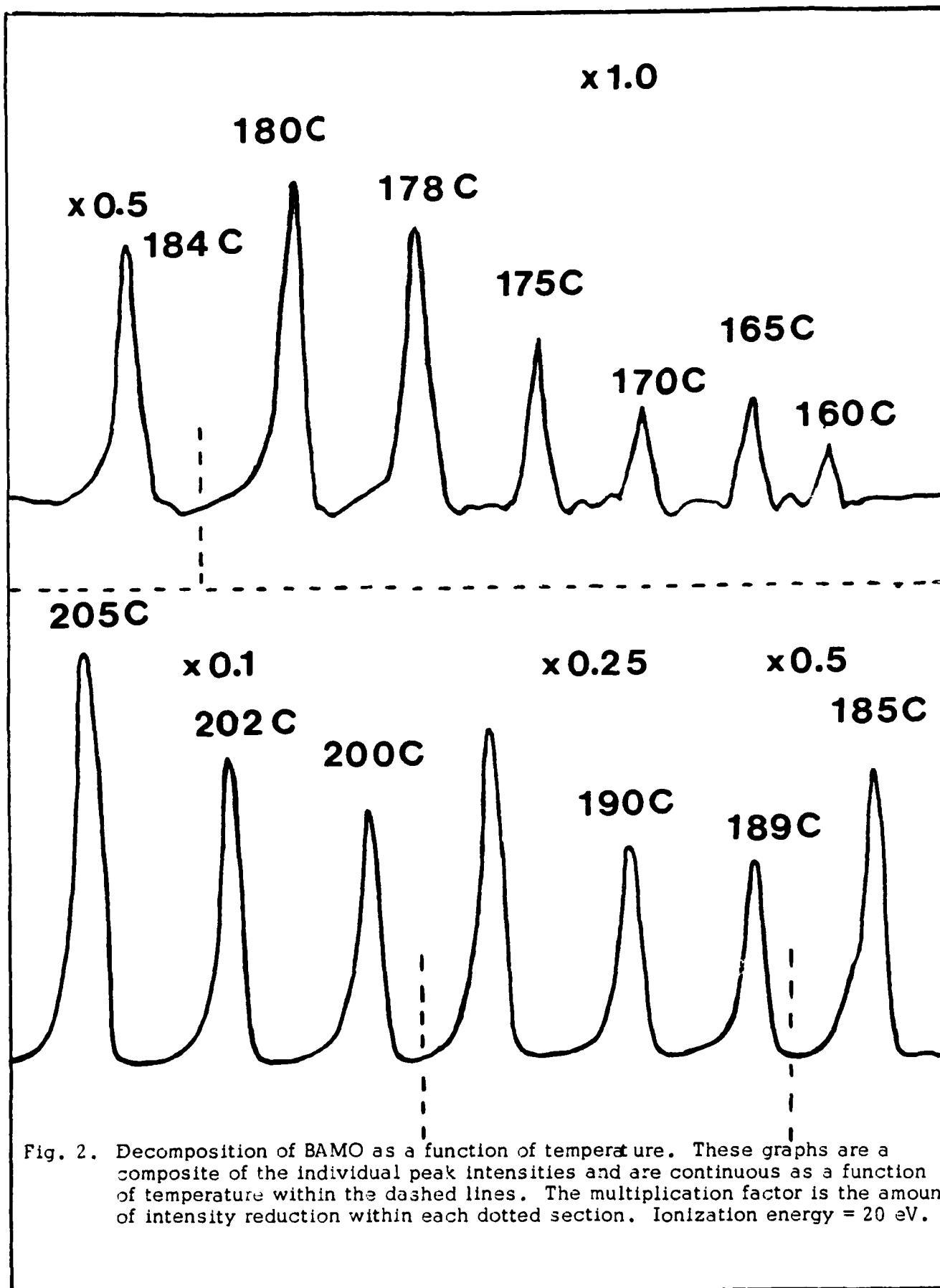


Fig. 2. Decomposition of BAMO as a function of temperature. These graphs are a composite of the individual peak intensities and are continuous as a function of temperature within the dashed lines. The multiplication factor is the amount of intensity reduction within each dotted section. Ionization energy = 20 eV.

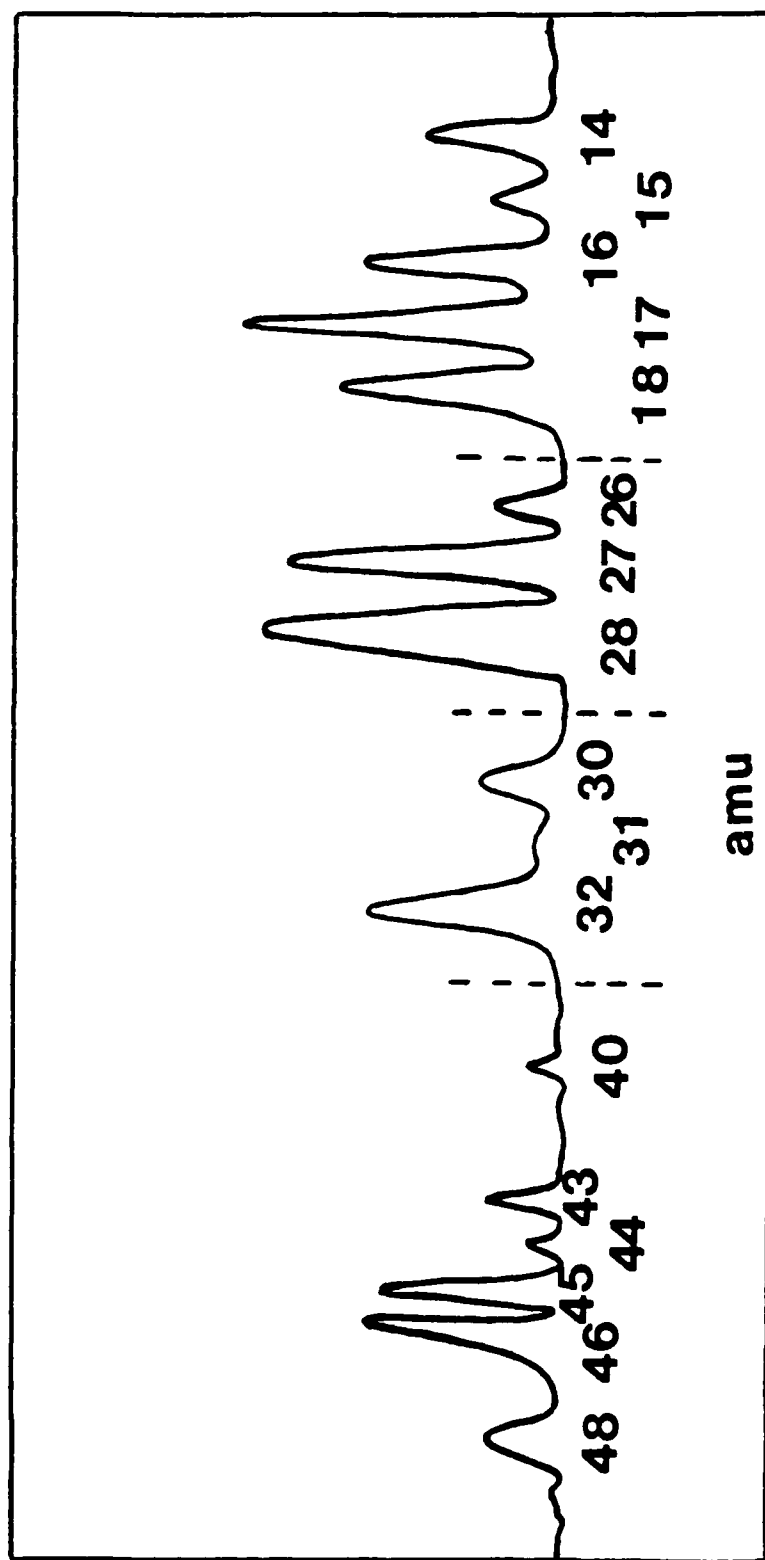


Fig. 3. Products from the thermal decomposition of BAMO at 200 C. Peak heights are only relative within the designated sections.

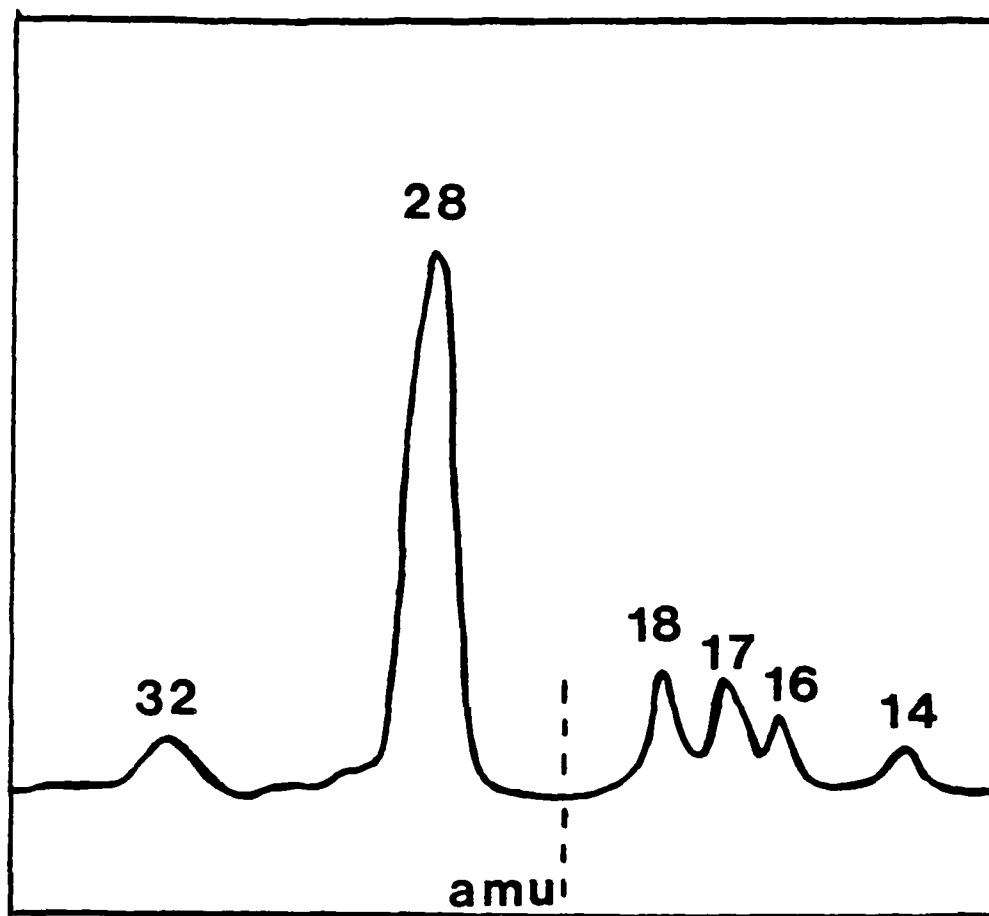


Fig. 4. Thermal decomposition of AMMO at 210 C. The azide group is decomposing, with the release of  $N_2$ . Some end group decomposition is also taking place; OH and  $H_2O$  peaks are observed at amu 17 and 18.

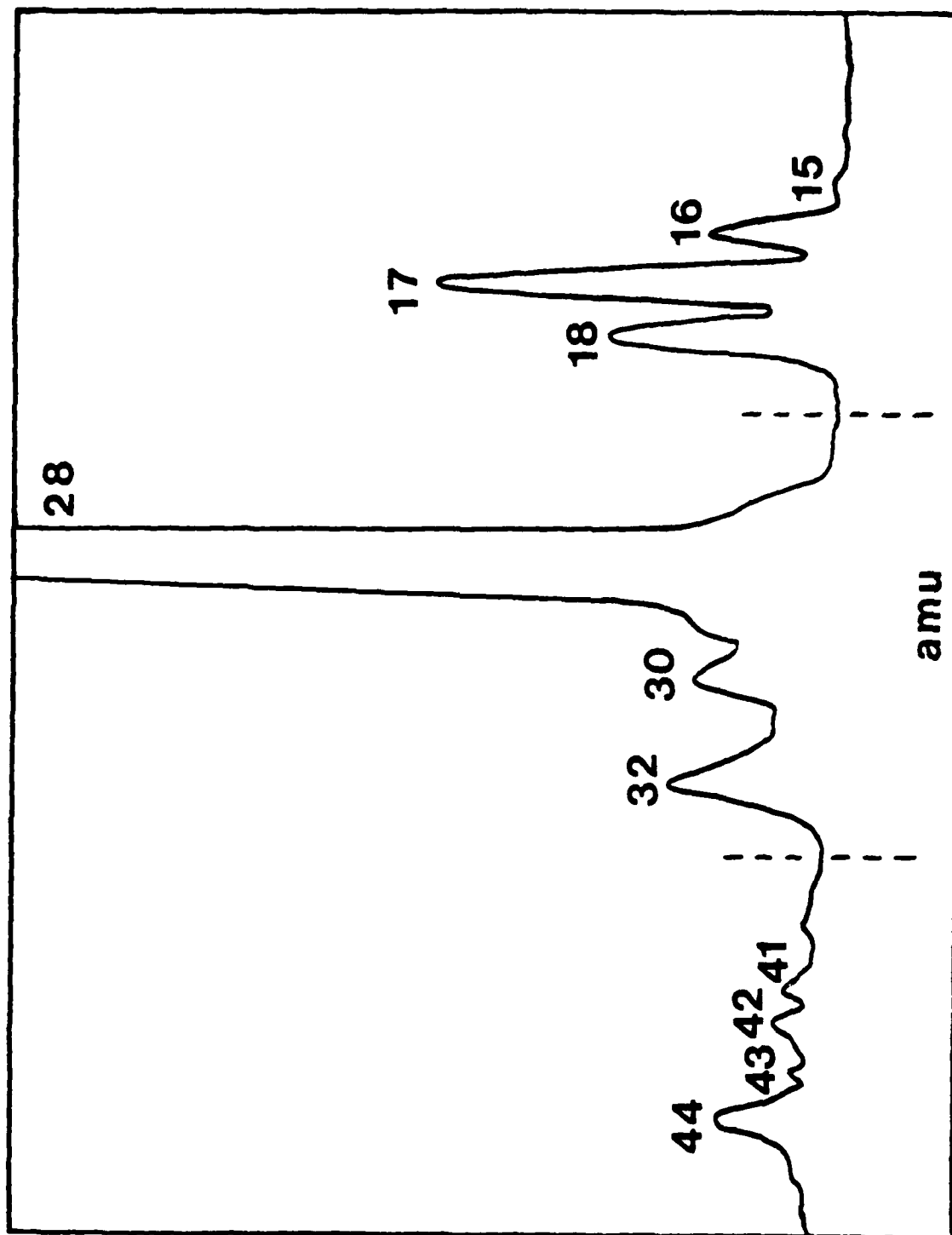


Fig. 5. AMMO products at 290 C In three amu ranges showing disintegration of the backbone

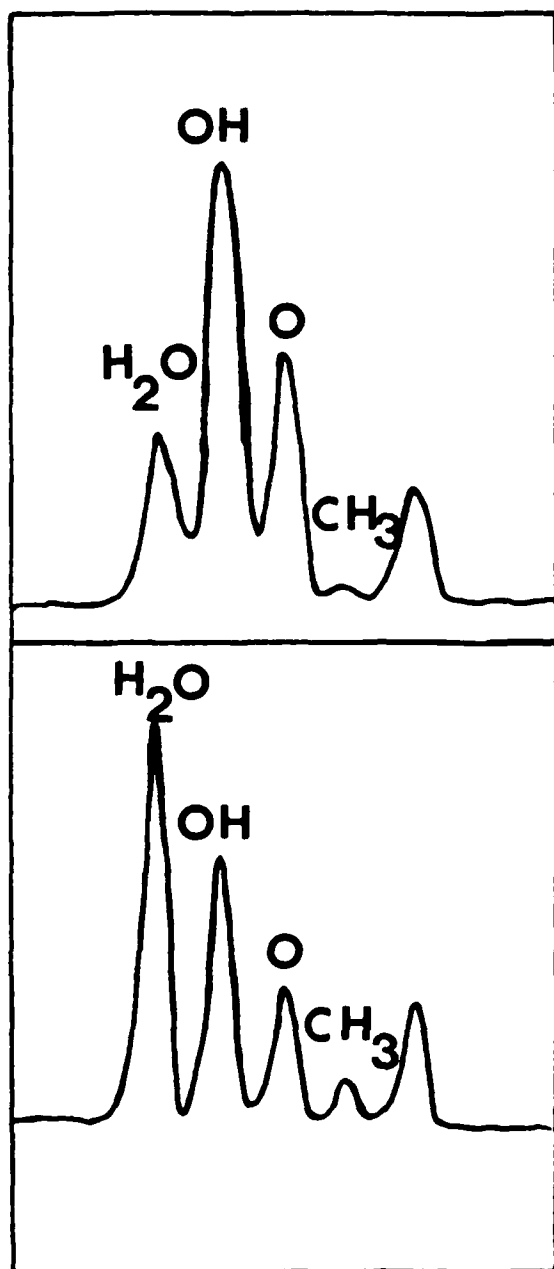


Fig. 6.a. Thermal decomposition comparison of AMMO (Part A) and BAMO (Part B) showing relative peaks of  $OH$ ,  $H_2O$  and  $CH_3$

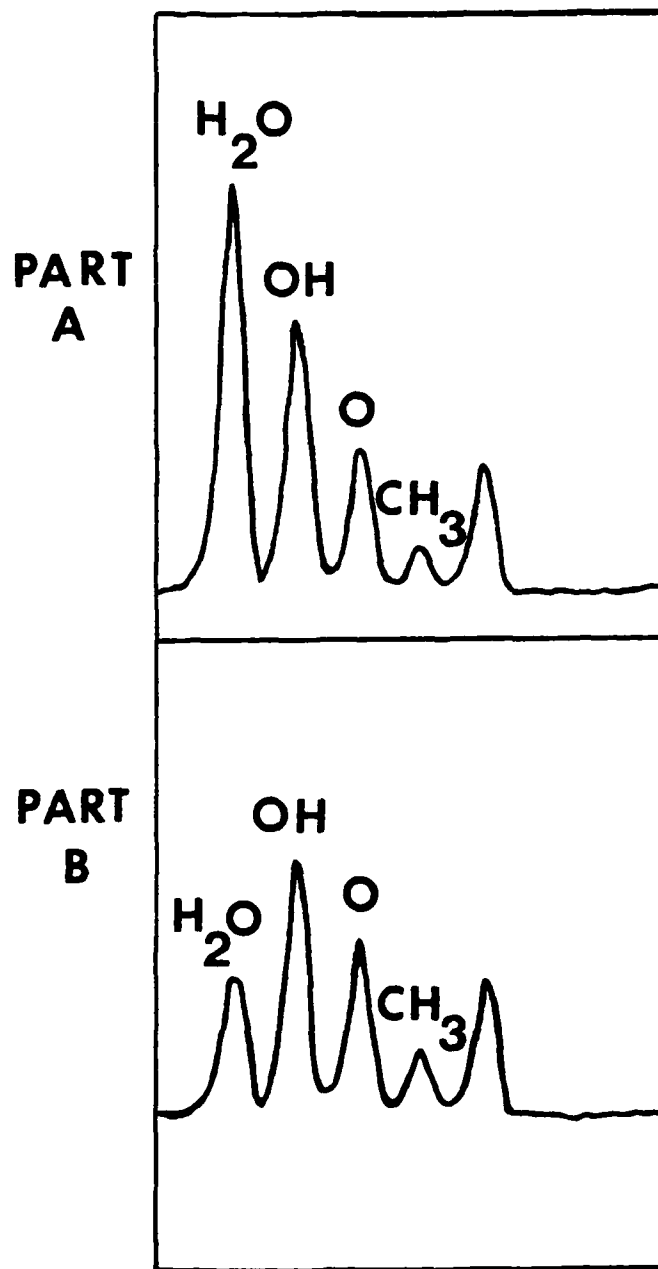


Fig. 6.b. Thermal decomposition comparison of BAMO at 235 C (Part A) and 215 C (Part B) showing the reversal of the relative concentration of  $OH$  and  $H_2O$  at 215 and 235 C

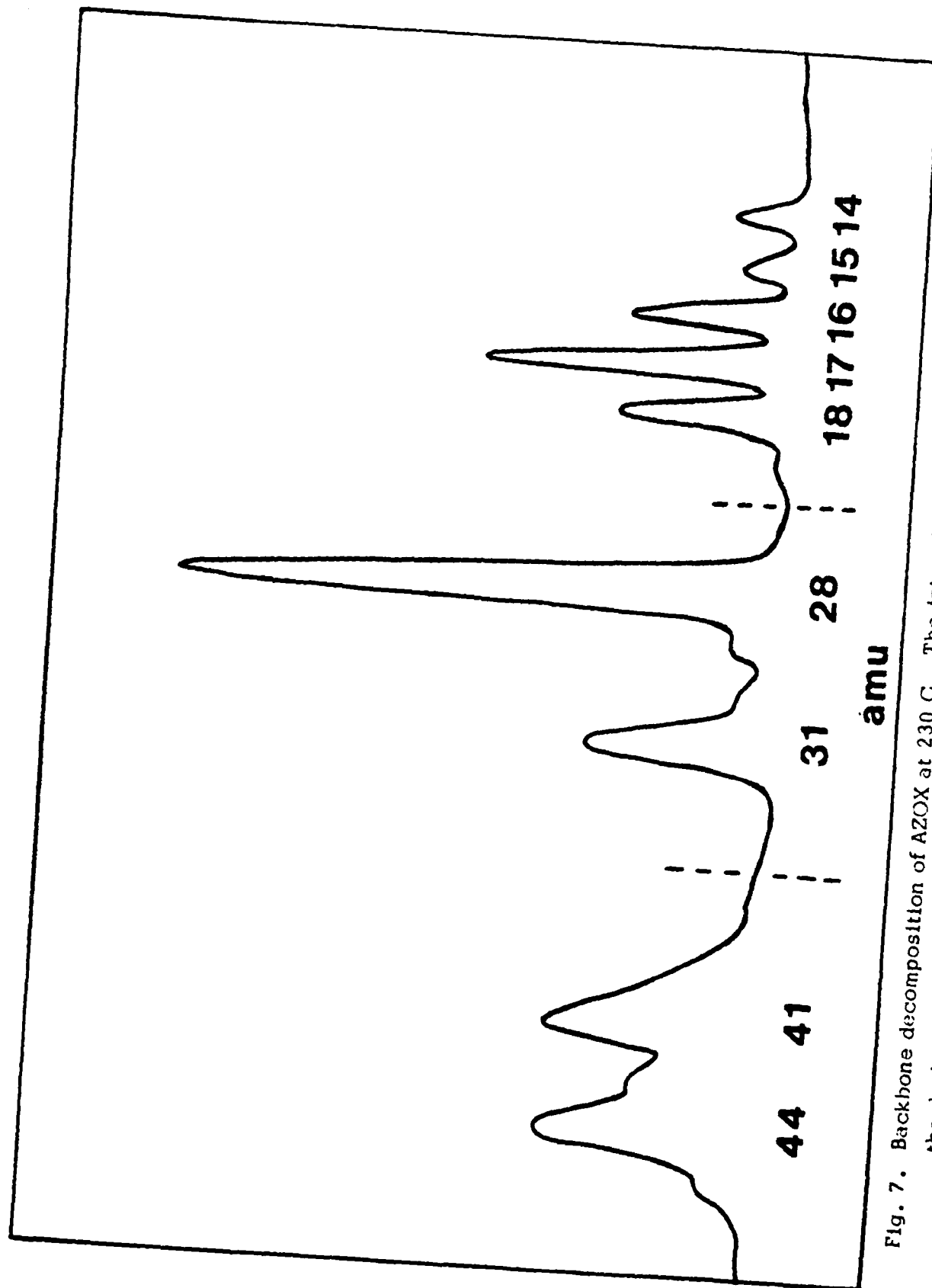


Fig. 7. Backbone decomposition of AZOX at 230 C. The intensities are continuous only within the dashed lines.

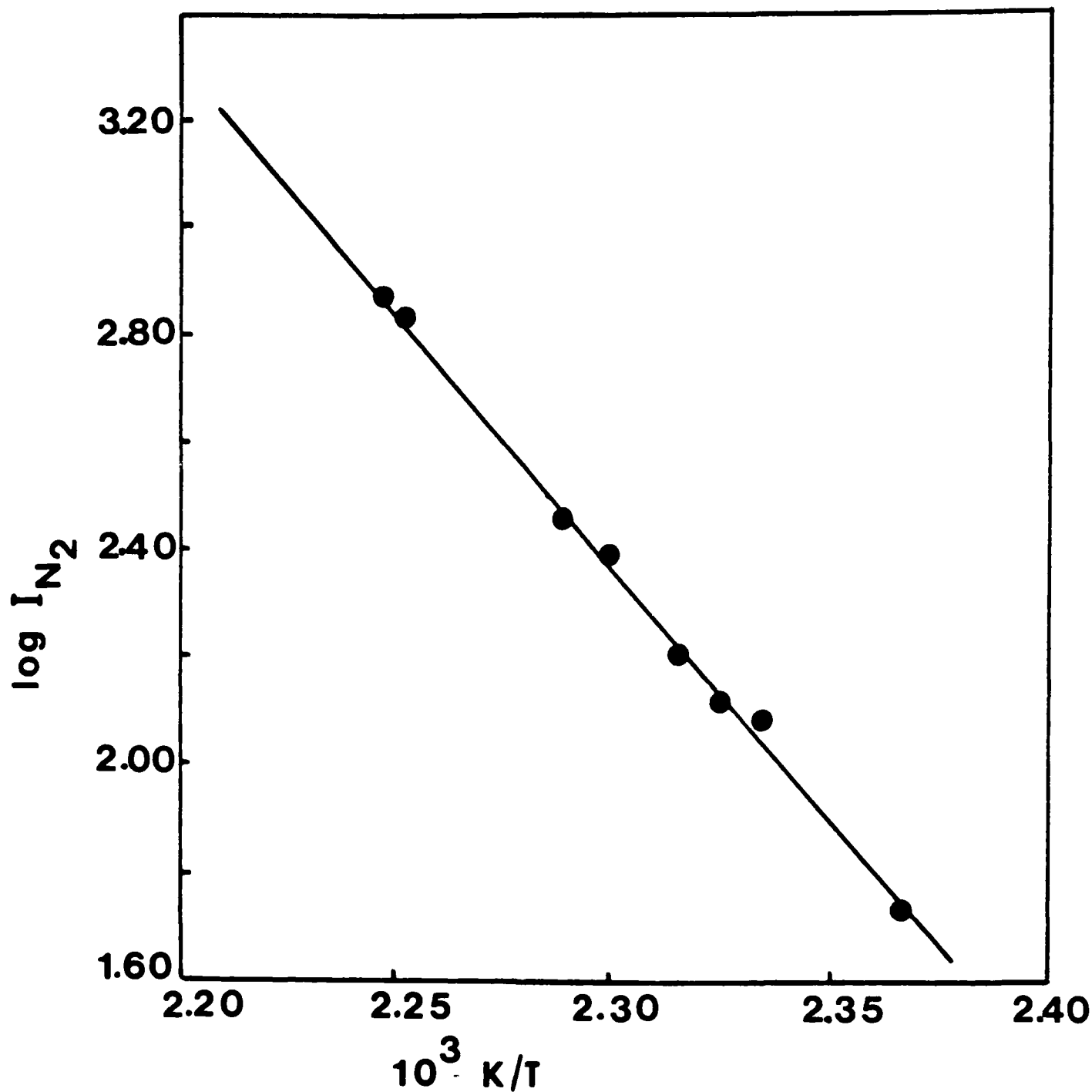


Fig. 8. Log of the relative intensity of  $N_2$  from the thermal decomposition of GAP plotted as a function of the reciprocal of the absolute temperature. Activation energy =  $176.6 \text{ kJ mol}^{-1}$  ( $42.2 \text{ kcal/mole}$ )



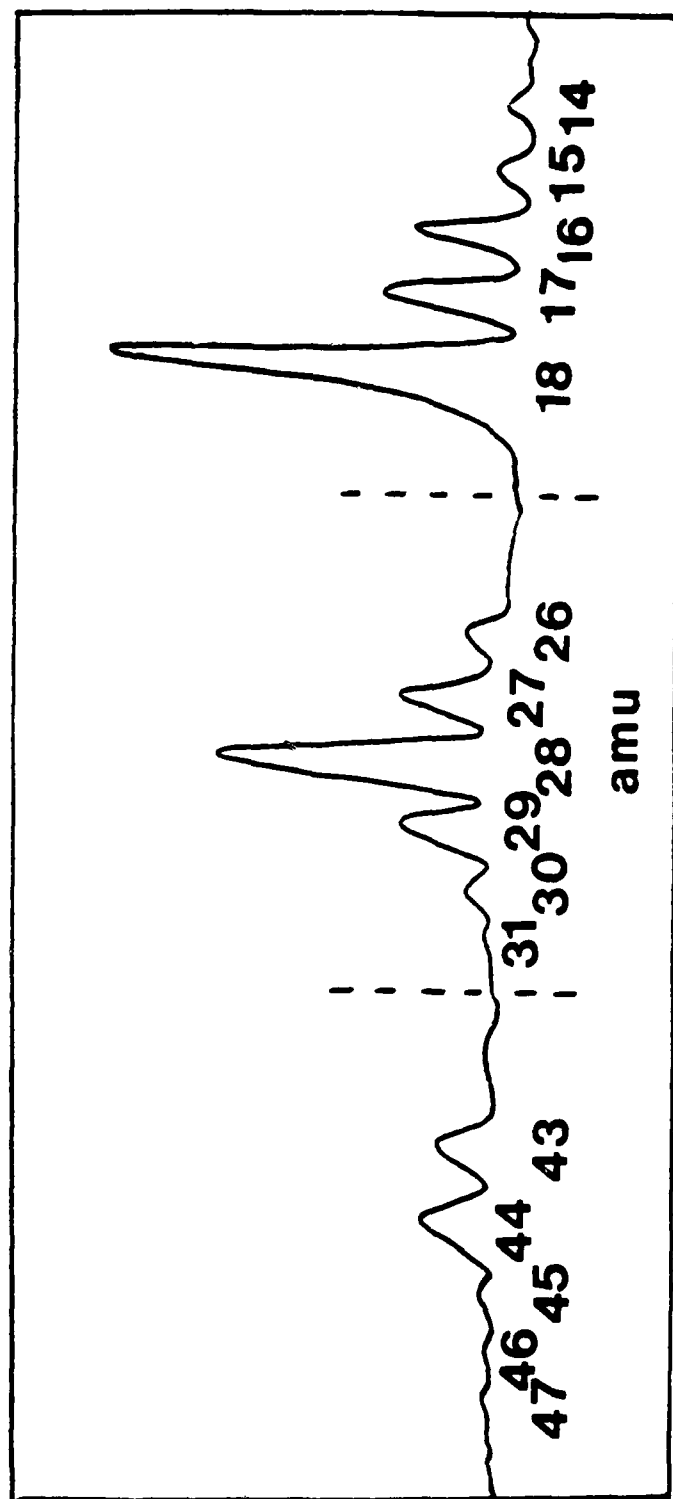


Fig. 9. Secondary decomposition products of GAP observed at 200 C. The intensities are continuous only within the dashed lines.

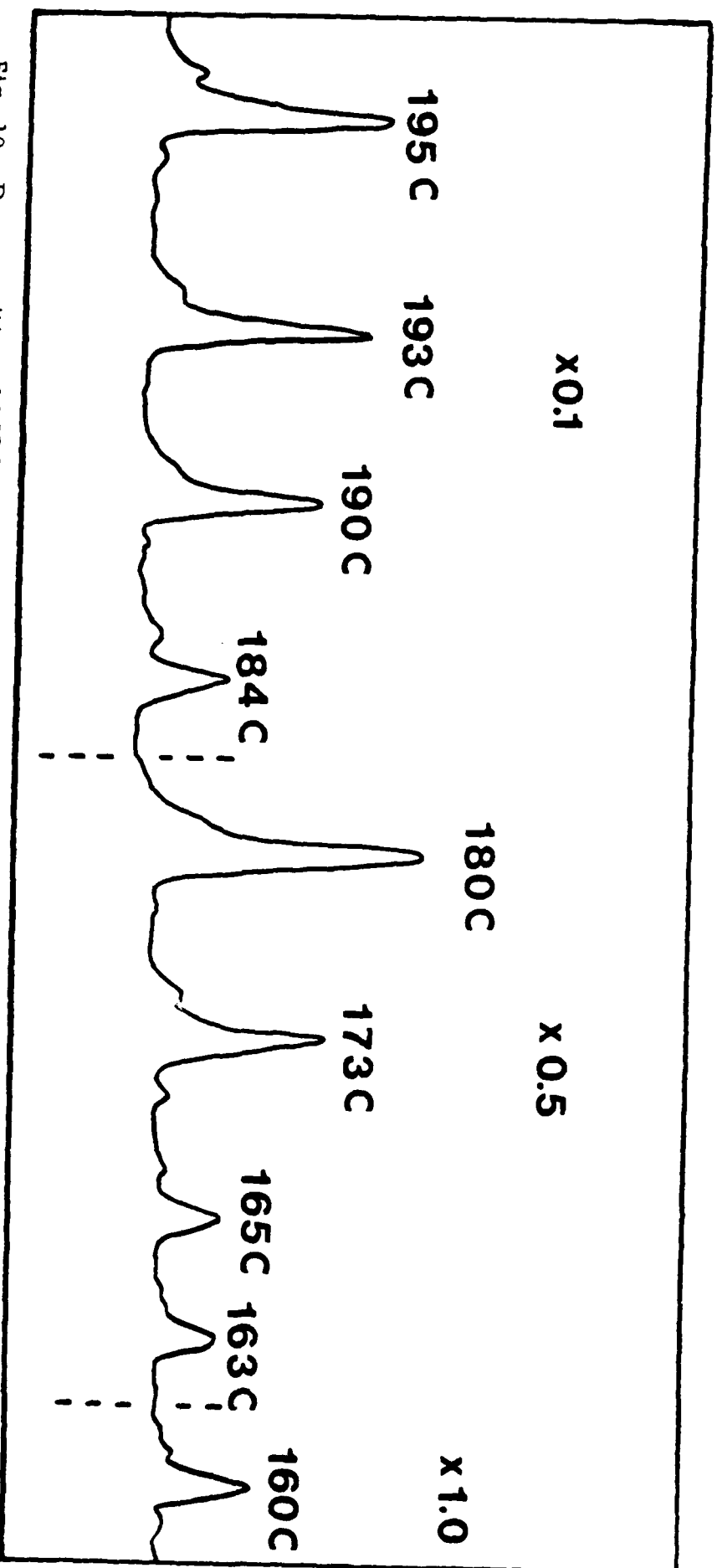


Fig. 10. Decomposition of AZOX monomer as a function of temperature with relative intensities of  $N_2$ . This is a composite of the individual peak heights and are continuous within the dashed lines as a function of temperature. Amu range = 24 to 32. The central peaks are molecular nitrogen, with smaller peaks on each side of HCN at 27 amu and HCO at 29 amu. The multiplication factor is the amount of intensity reduction within each dotted section.

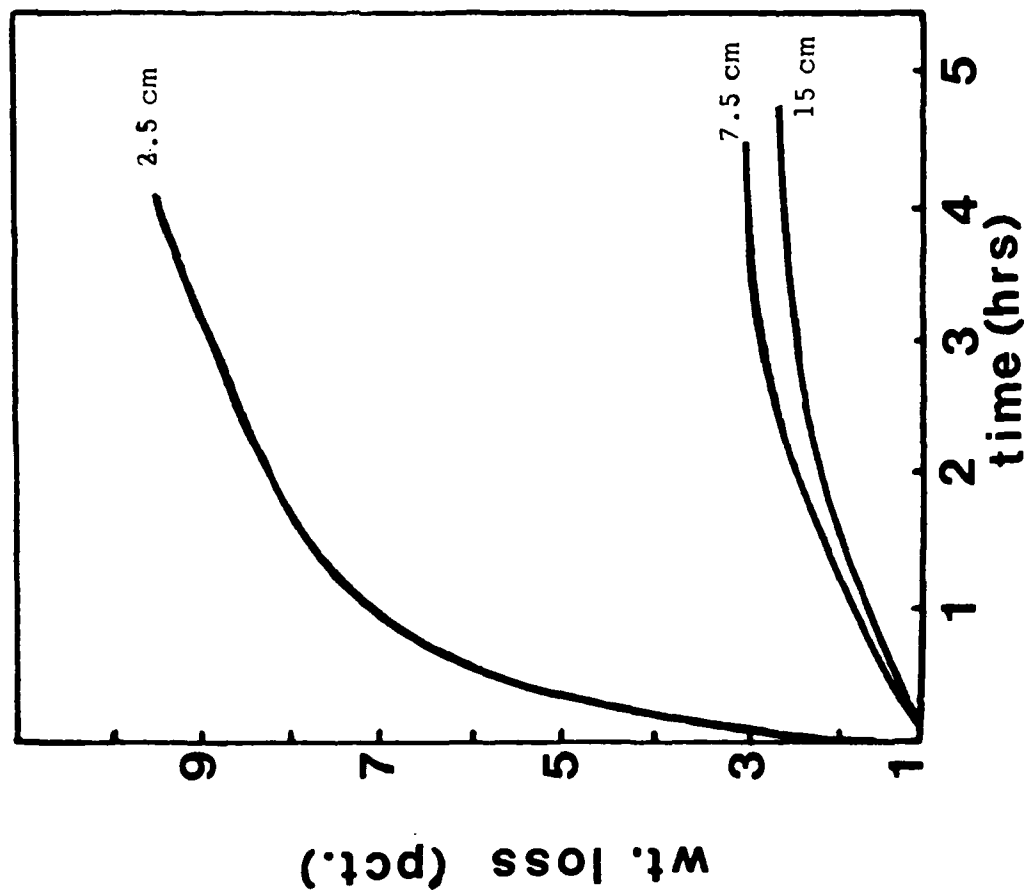


Fig. 11. Weight loss of AMMO homopolymer as a function of long wave (360 nm) ultraviolet radiation at distances of 2.5 cm (10,000  $\mu\text{watts}/\text{cm}^2$ ), 7.5 cm (1,120  $\mu\text{watts}/\text{cm}^2$ ), and 15 cm (380  $\mu\text{watts}/\text{cm}^2$ ) from the sample surface. The intensity of the radiation is 3.39 eV (78 kcal/mole)

INIT

DISTRIBUTION LIST

	<u>No. Copies</u>		<u>No. Copies</u>
Dr. L.V. Schmidt Assistant Secretary of the Navy (R,E, and S) Room 5E 731 Pentagon Washington, D.C. 20350	1	Dr. F. Roberto Code AFRPL MKPA Edwards AFB, CA 93523	1
Dr. A.L. Slafkosky Scientific Advisor Commandant of the Marine Corps Code RD-1 Washington, D.C. 20380	1	Dr. L.H. Caveny Air Force Office of Scientific Research Directorate of Aerospace Sciences Bolling Air Force Base Washington, D.C. 20332	1
Dr. Richard S. Miller Office of Naval Research Code 432 Arlington, VA 22217	10	Mr. Donald L. Ball Air Force Office of Scientific Research Directorate of Chemical Sciences Bolling Air Force Base Washington, D.C. 20332	1
Mr. David Siegel Office of Naval Research Code 260 Arlington, VA 22217	1	Dr. John S. Wilkes, Jr. FJSRL/NC USAF Academy, CO 80840	1
Dr. R.J. Marcus Office of Naval Research Western Office 1030 East Green Street Pasadena, CA 91106	1	Dr. R.L. Lou Aerojet Strategic Propulsion Co. P.O. Box 15699C Sacramento, CA 95813	1
Dr. Larry Peebles Office of Naval Research East Central Regional Office 666 Summer Street, Bldg. 114-D Boston, MA 02210	1	Dr. V.J. Keenan Anal-Syn Lab Inc. P.O. Box 547 Paoli, PA 19301	1
Dr. Phillip A. Miller Office of Naval Research Naval Station, Treasure Island Bldg. 7, Rm. 81 San Francisco, CA 94130	1	Dr. Philip Howe Army Ballistic Research Labs ARRADCOM Code DRDAR-BLT Aberdeen Proving Ground, MD 21005	1
Mr. Otto K. Heiney AFATL - DLDL Eglin AFB, FL 32542	1	Mr. L.A. Watermeier Army Ballistic Research Labs ARRADCOM Code DRDAR-BLI Aberdeen Proving Ground, MD 21005	1
Mr. R. Geisler ATTN: MKP/MS24 AFRPL Edwards AFB, CA 93523	1	Dr. W.W. Wharton Attn: DRSMI-RKL Commander U.S. Army Missile Command Redstone Arsenal, AL 35898	1

6/81

INIT

DISTRIBUTION LIST

	<u>No. Copies</u>		<u>No. Copies</u>
Mr. J. Murrin Naval Sea Systems Command Code 62R2 Washington, D.C. 20362	1	Dr. A. Nielsen Naval Weapons Center Code 385 China Lake, CA 93555	1
Dr. P.J. Pastine Naval Surface Weapons Center Code R04 White Oak Silver Spring, MD 20910	1	Dr. R. Reed, Jr. Naval Weapons Center Code 388 China Lake, CA 93555	1
Mr. L. Roslund Naval Surface Weapons Center Code R122 White Oak Silver Spring, MD 20910	1	Dr. L. Smith Naval Weapons Center Code 3205 China Lake, CA 93555	1
Mr. M. Stosz Naval Surface Weapons Center Code R121 White Oak Silver Spring, MD 20910	1	Dr. B. Douda Naval Weapons Support Center Code 5042 Crane, IN 47522	1
Dr. E. Zimmet Naval Surface Weapons Center Code R13 White Oak Silver Spring, MD 20910	1	Dr. A. Faulstich Chief of Naval Technology MAT Code 0716 Washington, D.C. 20360	1
Dr. D.R. Derr Naval Weapons Center Code 388 China Lake, CA 93555	1	LCDR J. Walker Chief of Naval Material Office of Naval Technology MAT, Code 0712 Washington, D.C. 20360	1
Mr. Lee N. Gilbert Naval Weapons Center Code 3205 China Lake, CA 93555	1	Mr. Joe McCartney Naval Ocean Systems Center San Diego, CA 92152	1
Dr. E. Martin Naval Weapons Center Code 3858 China Lake, CA 93555	1	Dr. S. Yamamoto Marine Sciences Division Naval Ocean Systems Center San Diego, CA 91232	1
Mr. R. McCarten Naval Weapons Center Code 3272 China Lake, CA 93555	1	Dr. G. Bosmajian Applied Chemistry Division Naval Ship Research & Development Center Annapolis, MD 21401	1
		Dr. H. Shuey Rohm and Haas Company Huntsville, AL 35801	1

INIT

DISTRIBUTION LIST

	<u>No. Copies</u>		<u>No. Copies</u>
Mr. R. Brown Naval Air Systems Command Code 330 Washington, D.C. 20361	1	Dr. J. Schnur Naval Research Lab. Code 6510 Washington, D.C. 20375	1
Dr. H. Rosenwasser Naval Air Systems Command AIR-310C Washington, D.C. 20360	1	Mr. R. Beauregard Naval Sea Systems Command SEA 64E Washington, D.C. 20362	1
Mr. B. Sobers Naval Air Systems Command Code 03P25 Washington, D.C. 20360	1	Mr. G. Edwards Naval Sea Systems Command Code 62R3 Washington, D.C. 20362	1
Dr. L.R. Rothstein Assistant Director Naval Explosives Dev. Engineering Dept. Naval Weapons Station Yorktown, VA 23691	1	Mr. John Boyle Materials Branch Naval Ship Engineering Center Philadelphia, PA 19112	1
Dr. Lionel Dickinson Naval Explosive Ordnance Disposal Tech. Center Code D Indian Head, MD 20640	1	Dr. H.G. Adolph Naval Surface Weapons Center Code R11 White Oak Silver Spring, MD 20910	1
Mr. C.L. Adams Naval Ordnance Station Code PM4 Indian Head, MD 20640	1	Dr. T.D. Austin Naval Surface Weapons Center Code R16 Indian Head, MD 20640	1
Mr. S. Mitchell Naval Ordnance Station Code 5253 Indian Head, MD 20640	1	Dr. T. Hall Code R-11 Naval Surface Weapons Center White Oak Laboratory Silver Spring, MD 20910	1
Dr. William Tolles Dean of Research Naval Postgraduate School Monterey, CA 93940	1	Mr. G.L. Mackenzie Naval Surface Weapons Center Code R101 Indian Head, MD 20640	1
Naval Research Lab. Code 6100 Washington, D.C. 20375	1	Dr. K.F. Mueller Naval Surface Weapons Center Code R11 White Oak Silver Spring, MD 20910	1

DISTRIBUTION LIST

	<u>No. Copies</u>		<u>No. Copies</u>
Dr. R.G. Rhoades Commander Army Missile Command DRSMI-R Redstone Arsenal, AL 35898	1	Dr. E.H. Debutts Hercules Inc. Baccus Works P.O. Box 98 Magna, UT 84044	1
Dr. W.D. Stephens Atlantic Research Corp. Pine Ridge Plant 7511 Wellington Rd. Gainesville, VA 22065	1	Dr. James H. Thacher Hercules Inc. Magna Baccus Works P.O. Box 98 Magna, UT 84044	1
Dr. A.W. Barrows Ballistic Research Laboratory USA ARRADCOM DRDAR-BLP Aberdeen Proving Ground, MD 21005	1	Mr. Theodore M. Gilliland Johns Hopkins University APL Chemical Propulsion Info. Agency Johns Hopkins Road Laurel, MD 20810	1
Dr. C.M. Frey Chemical Systems Division P.O. Box 358 Sunnyvale, CA 94086	1	Dr. R. McGuire Lawrence Livermore Laboratory University of California Code L-324 Livermore, CA 94550	1
Professor F. Rodriguez Cornell University School of Chemical Engineering Olin Hall Ithaca, NY 14853	1	Dr. Jack Linsk Lockheed Missiles & Space Co. P.O. Box 504 Code Org. 83-10, Bldg. 154 Sunnyvale, CA 94088	1
Defense Technical Information Center DTIC-DDA-2 Cameron Station Alexandria, VA 22314	12	Dr. B.G. Craig Los Alamos National Lab P.O. Box 1663 NSP/DOD, MS-245 Los Alamos, NM 87545	1
		Dr. R.L. Rabie WX-2, MS-952 Los Alamos National Lab. P.O. Box 1663 Los Alamos, NM 87545	1
Dr. Ronald L. Simmons Hercules Inc. Eglin AFATL/DL DL Eglin AFB, FL 32542	1	Dr. R. Rogers Los Alamos Scientific Lab. WX-2 P.O. Box 1663 Los Alamos, NM 87545	1

6/81

## DISTRIBUTION LIST

	<u>No. Copies</u>		<u>No. Copies</u>
Dr. J.F. Kincaid Strategic Systems Project Office Department of the Navy Room 901 Washington, D.C. 20376	1	Dr. C.W. Vriesen Thiokol Elkton Division P.O. Box 241 Elkton, MD 21921	1
Strategic Systems Project Office Propulsion Unit Code SP2731 Department of the Navy Washington, D.C. 20376	1	Dr. J.C. Hinshaw Thiokol Wasatch Division P.O. Box 524 Brigham City, UT 83402	1
Mr. E.L. Throckmorton Strategic Systems Project Office Department of the Navy Room 1048 Washington, D.C. 20376	1	U.S. Army Research Office Chemical & Biological Sciences Division P.O. Box 12211 Research Triangle Park, NC 27709	1
Dr. D.A. Flanigan Thiokol Huntsville Division Huntsville, AL 35807	1	Dr. R.F. Walker USA ARRADCOM DRDAR-LCE Dover, NJ 07801	1
Mr. G.F. Mangum Thiokol Corporation Huntsville Division Huntsville, AL 35807	1	Dr. T. Sinden Munitions Directorate Propellants and Explosives Defense Equipment Staff British Embassy 3100 Massachusetts Ave. Washington, D.C. 20008	1
Mr. E.S. Sutton Thiokol Corporation Elkton Division P.O. Box 241 Elkton, MD 21921	1	Mr. J.M. Frankle Army Ballistic Research Labs ARRADCOM Code DRDAR-BLI Aberdeen Proving Ground, MD 21005	1
Dr. G. Thompson Thiokol Wasatch Division MS 240 P.O. Box 524 Brigham City, UT 84302	1	Dr. Ingo W. May Army Ballistic Research Lab ARRADCOM Code DRDAR-BLI Aberdeen Proving Ground, MD 21005	1
Dr. T.F. Davidson Technical Director Thiokol Corporation Government Systems Group P.O. Box 9258 Ogden, UT 84409	1		



INIT

6/81

DISTRIBUTION LIST

	<u>No. Copies</u>		
E. J. Palm Commander Army Missile Command DRSMI-RK Redstone Arsenal, AL 35898	1	Dr. Kenneth O. Hartman Hercules Aerospace Division Hercules Incorporated Allegany Ballistics Lab P.O. Box 210 Cumberland, MD 21502	1
Dr. Merrill K. King Atlantic Research Corp. 5390 Cherokee Avenue Alexandria, VA 22314	1	Dr. Joyce J. Kaufman The Johns Hopkins University Department of Chemistry Baltimore, MD 21218	1
Dr. R.J. Bartlett Batelle Columbus Laboratories 505 King Avenue Columbus, OH 43201	1	Dr. John K. Dienes T-3, MS-216 Los Alamos National Lab P.O. Box 1663 Los Alamos, NM 87544	1
Dr. P. Rentzepis Bell Laboratories Murray Hill, NJ 07971	1	Dr. H.P. Marshall Dept. 52-35, Bldg. 204.2 Lockheed Missile & Space Co. 3251 Hanover Street Palo Alto, CA 94304	1
Professor Y.T. Lee Department of Chemistry University of California Berkeley, CA 94720	1	Professor John Deutsch MIT Department of Chemistry Cambridge, MA 02139	1
Professor M. Nicol Department of Chemistry 405 Hilgard Avenue University of California Los Angeles, CA 90024	1	Professor Barry Kunz College of Sciences & Arts Department of PHysics Michigan Technological Univ. Houghton, MI 49931	1
Professor S.S. Penner University of California Energy Center Mail Code B-010 La Jolla, CA 92093	1	Dr. R. Bernecker Code R13 Naval Surface Weapons Center White Oak Silver Spring, MD 20910	1
Professor Curt Wittig University of Southern CA Dept. of Electrical Engineering University Park Los Angeles, CA 90007	1	Dr. C.S. Coffey Naval Surface Weapons Center Code R13 White Oak Silver Spring, MD 20910	1

INIT

6/81

DISTRIBUTION LIST

	<u>No. Copies</u>
Dr. W. L. Elban Code R13 Naval Surface Weapons Center White Oak Silver Spring, MD 20910	1
Mr. K.J. Graham Naval Weapons Center Code 3835 China Lake, CA 93555	1
Dr. B. Junker Office of Naval Research Code 421 Arlington, VA 22217	1
Prof. H.A. Rabitz Department of Chemistry Princeton University Princeton, NH 08540	1
Dr. M. Farber Space Sciences, Inc. 135 West Maple Avenue Monrovia, CA 91016	1
Mr. M. Hill SRI International 333 Ravenswood Avenue Menlo Park, CA 94025	1
U.S. Army Research Office Engineering Division Box 12211 Research Triangle Park, NC 27709	1
U.S. Army Research Office Metallurgy & Materials Sci. Div. Box 12211 Research Triangle Park, NC 27709	1
Professor G.D. Duvall Washington State University Department of Physics Pullman, WA 99163	1